XIIIth School of Cosmology

November 12 - 18, 2017 — IESC, Cargèse

The CMB from A to Z

promises and challenges of the CMB as a cosmological probe

Primordial non-Gaussianity

Sabino Matarrese

Physics & Astronomy Dept. “G. Galilei”, University of Padova, Italy

INFN, Sezione di Padova

INAF, Osservatorio Astronomico di Padova

GSSI, L’Aquila, Italy

The Gaussian hypothesis in Cosmology

- "That a Gaussian random field may provide a good description of the properties of density fluctuations could arise in a number of ways. The central limit theorem implies that a Gaussian distribution arises whenever one has a variable (or, more generally, a vector) which is a linear superposition of a large number of independent random variables (or vectors) which are all drawn from the same distribution. In particular, if the field F(r) is written as a spatial Fourier decomposition, and its Fourier coefficients F_k are statistically independent, each having the same form of distribution, then the joint probability of the density evaluated at a finite number of points will be Gaussian under very weak conditions. Special cases of this include the random phase approximation, in which it is assumed that the phases of F_k are uniformly distributed from 0 to 2π. The specific form of the distribution of the moduli $|F_k|$ does not matter. We note that small-amplitude curvature perturbations generated by quantum fluctuations in an inflationary phase of the very early universe would yield a Gaussian random density field. …" (Bardeen, Bond, Kaiser & Szalay 1986).

Why (non-) Gaussian?

Gaussian

free (i.e. non-interacting) field

large-scale phase coherence

non-linear gravitational dynamics

The phase information

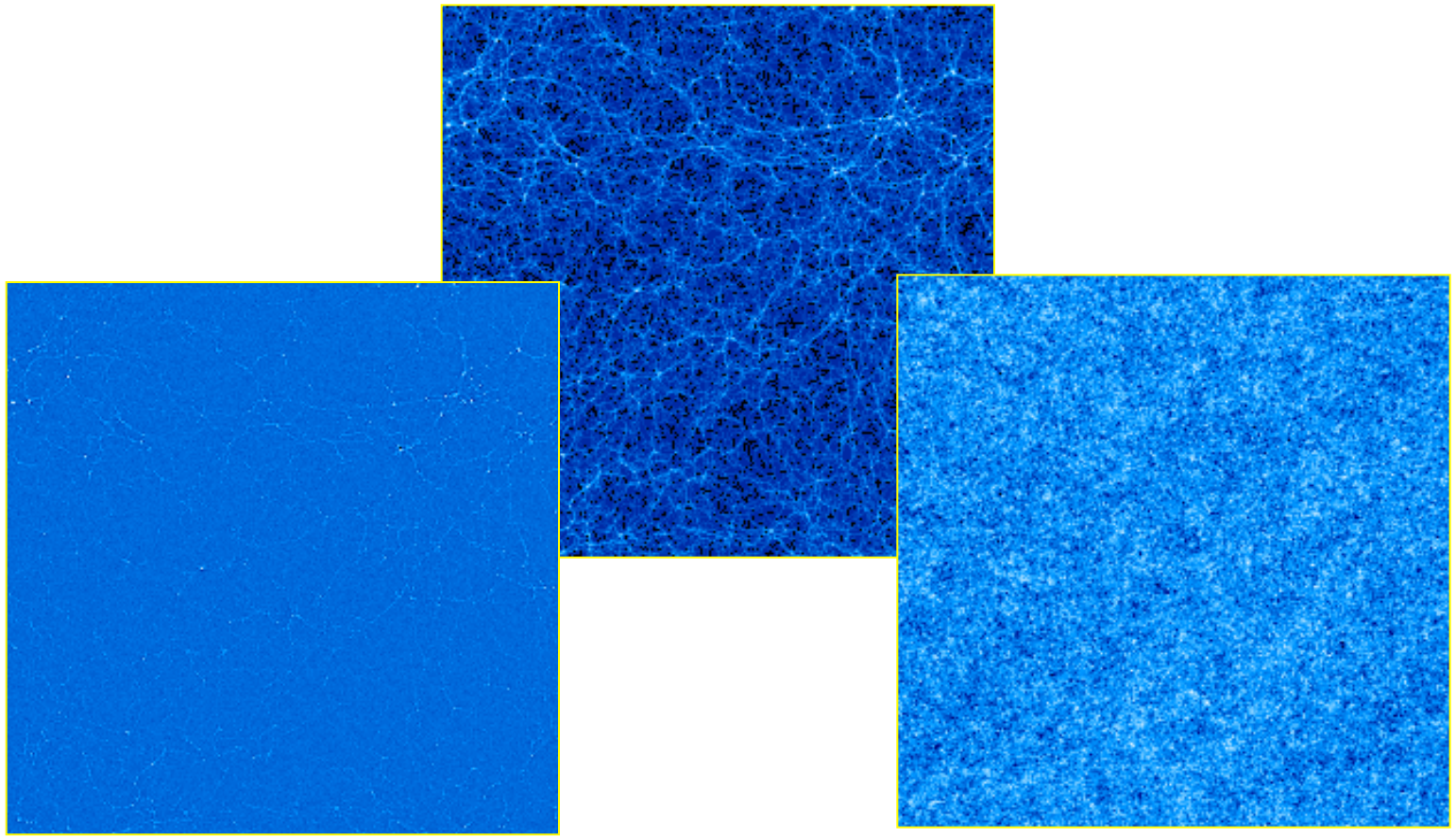

credits: *Peter Coles*

Going beyond the Gaussian hypothesis in Cosmology

Historical outline:

1977 Groth & Peebles compute the 3-pt function of galaxies: direct evidence that the LSS is non-Gaussian. Is this only the effect of non-linear gravitational clustering?

1980 Strongly non-Gaussian initial conditions studied in the eighties. Perturbation theory calculations beyond the linear level compute bispectrum, skewness, etc. using the Newtonian approximation (both in Eulerian and Lagrangian coordinates (Bouchet et al. 1995; Catelan et al. 1995; …), starting from Gaussian and in a few cases also NG initial conditions.

2001 Determination of bispectrum for PSCz (Feldman et al. 2001) and 2dF galaxies (Verde et al. 2002).

1990 New era with f_{NL} non-Gaussian (NG) models from inflation (Salopek & Bond 1991; Gangui et al. 1994: $f_{NL} \sim 10^{-2}$; Verde et al. 1999; Komatsu & Spergel 2001; Acquaviva et al. 2002; Maldacena 2002; + many models with higher f_{NL}).

2000 Primordial NG (PNG) gradually emerged as a new "smoking gun" of (non-standard) inflation models, which complements the search for primordial gravitational waves (PGW). PNG probes interactions among fields at the highest energy scales.

2013 Is this route still viable, given the very stringent Planck constraints?

The view on Non-Gaussianity … circa 1990

Moscardini, Lucchin, Matarrese & Messina 1991

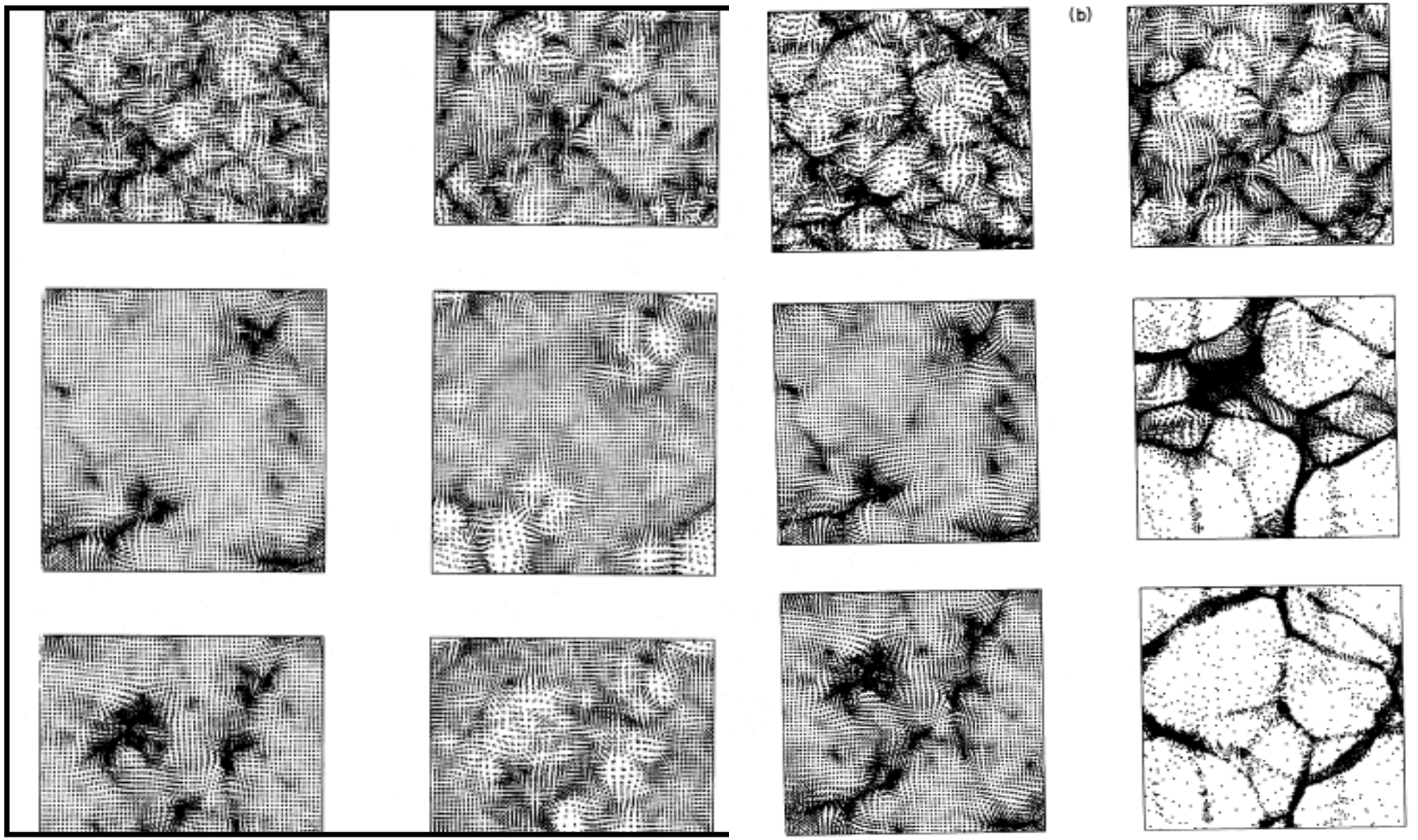

The present view on non-Gaussianity

- ✓ Alternative structure formation models of the late eighties considered strongly non-Gaussian primordial fluctuations.
- ✓ The increased accuracy in CMB and LSS observations has, however, excluded this extreme possibility.
- ✓ The present-day challenge is either detect or constrain mild or weak deviations from primordial Gaussian initial conditions.
- ✓ Deviations of this type are not only possible but are generically predicted in the standard perturbation generating mechanism provided by inflation.

Evaluating NG: from inflation to the present universe

Evaluate non-Gaussianity during inflation by a self-consistent second-order calculation (or equivalent techniques, …).

Evolve scalar (vector) and tensor perturbations to second order after inflation outside the horizon, matching conserved second-order gauge-invariant variable, such as the comoving curvature perturbation $\zeta^{(2)}$ (or non-linear generalizations of it), to its value at the end of inflation (accurately accounting for reheating).

Evolve them consistently after they re-enter the Hubble radius → i.e. compute second-order radiation transfer function for CMB and second-order matter transfer function for LSS (few codes already available!)

Non-Gaussianity in the Initial Conditions

Testable predictions of inflation

- Cosmological aspects
  - Critical density Universe
  - Almost scale-invariant and **nearly Gaussian**, adiabatic density fluctuations
  - Almost scale-invariant stochastic background of relic gravitational waves
- Particle physics aspects
  - **Nature of the inflaton**
  - Inflation energy scale

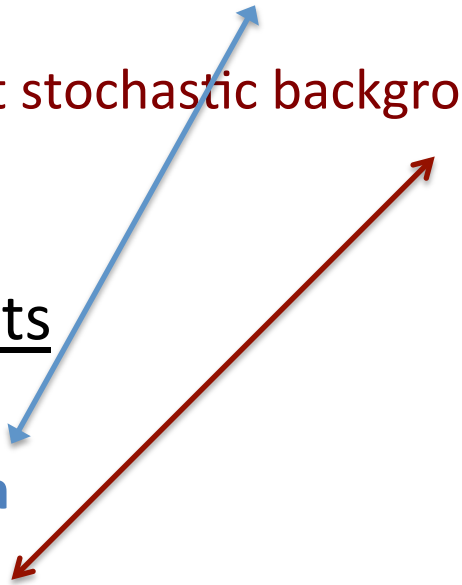

The rise and fall … of the comoving Hubble horizon

(late-time dark energy dominance neglected for simplicity)

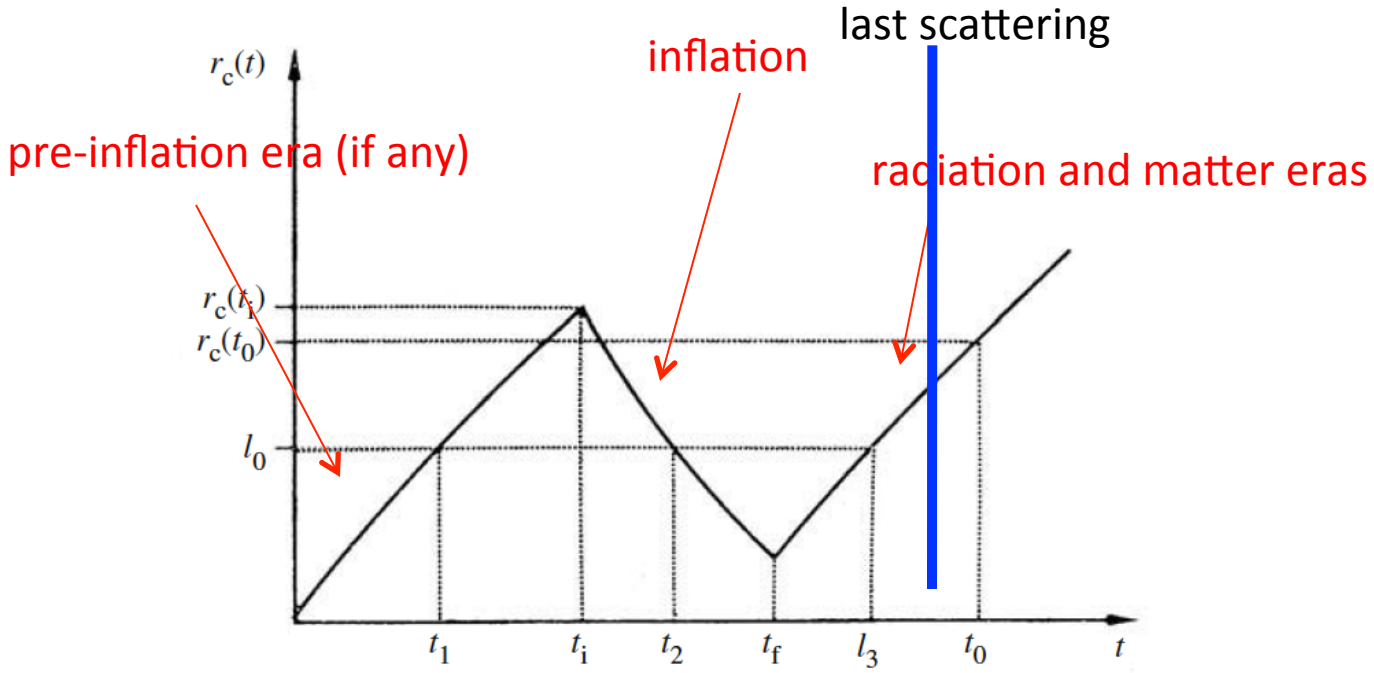

Figure 7.4 Evolution of the comoving cosmological horizon $r_c(t)$ in a universe characterised by a phase with an accelerated expansion (inflation) from t_i to t_f. The scale l_0 enters the horizon at t_1, leaves at t_2 and re-enters at t_3. In a model without inflation the horizon scale would never decrease so scales entering at t_0 could never have been in causal contact before. The horizon problem is resolved if $r_c(t_0) \leqslant r_c(t_i)$.

Inflation and the Inflaton

$$\mathcal{L}_\phi[\phi, g_{\mu\nu}] = \frac{1}{2} g^{\mu\nu} \phi_{,\mu} \phi_{,\nu} - V(\phi)$$

Standard kinetic term

Inflaton potential: describes the self-interactions of the inflaton field and its interactions with the rest of the world

Think the inflaton mean field as a particle moving under a force induced by the potential V

Ex: $V(\phi) = \frac{m^2}{2}\phi^2$

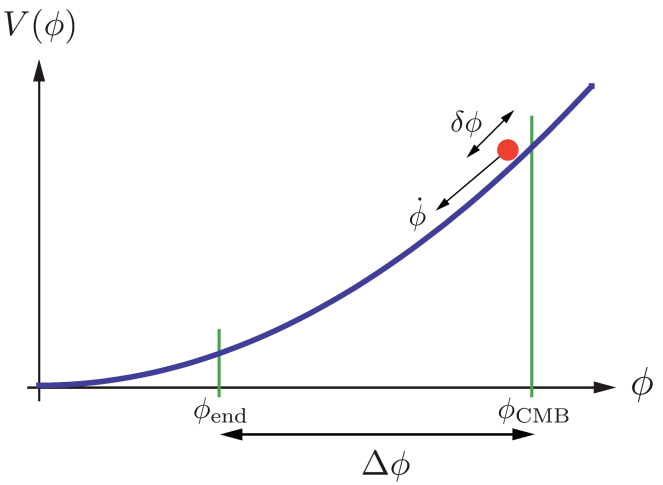

Two simple but very important examples

``Large field'' models

$$V(\phi) \propto \phi^{\alpha}$$

typical of ``caothic inflation scenario'' (Linde `83)

$$V(\phi) \propto \exp[\phi/\mu]$$

``power law inflation'' (Lucchin, Matarrese '85)

``Small field'' models

$$V(\phi) = V_0 \left[1 - \left(\frac{\phi}{\mu}\right)^p\right] \qquad \phi < \mu < M_{\rm Pl}$$

from spontaneous symmetry breaking or Goldstone, axion models (Linde; Albrecht, Steinhardt `82; Freese et al '90)

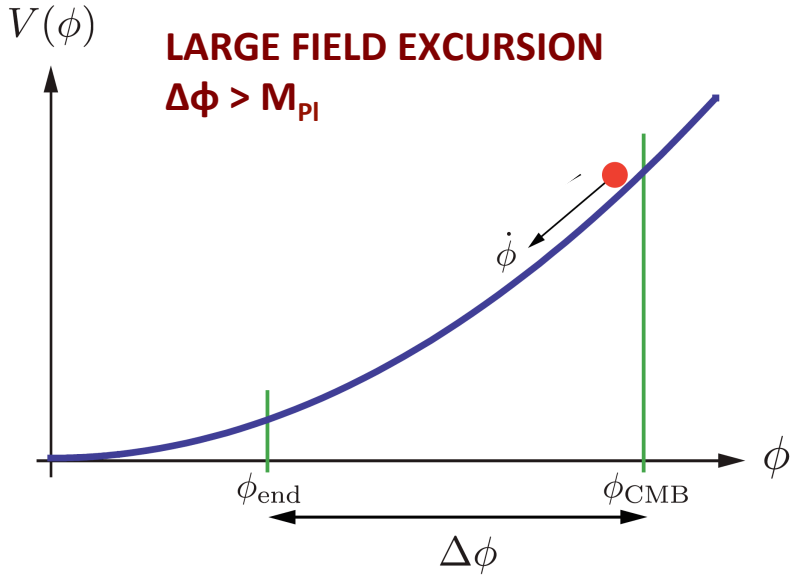

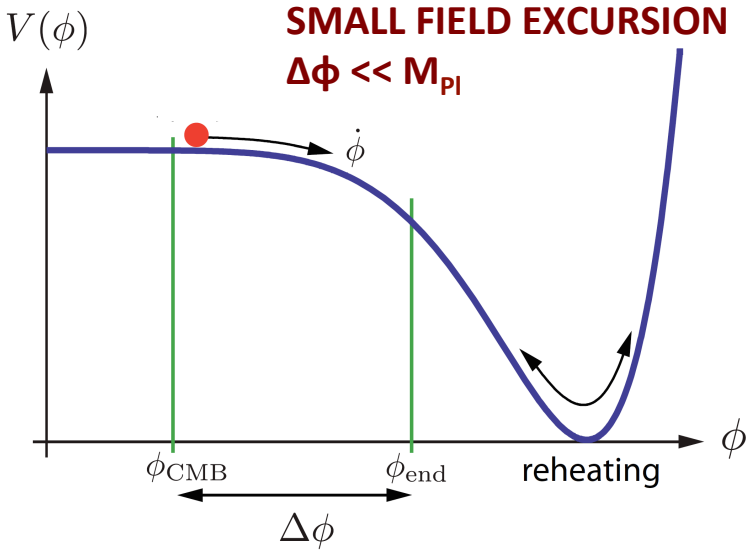

Observational predictions of inflation

- **Primordial density (scalar) perturbations**

$$\mathcal{P}_\zeta(k) = \frac{16}{9}\frac{V^2}{M_{\rm Pl}^4\dot{\phi}^2}\left(\frac{k}{k_0}\right)^{n-1}$$

spectral index: $n-1 = 2\eta - 6\epsilon$
(or ``tilt'')

amplitude

$$\epsilon = \frac{M_{\rm Pl}^2}{16\pi}\left(\frac{V'}{V}\right)^2 \ll 1;\ \eta = \frac{M_{\rm Pl}^2}{8\pi}\left(\frac{V''}{V}\right) \ll 1$$

- **Primordial (tensor) gravitational waves**

$$\mathcal{P}_{\rm T}(k) = \frac{128}{3}\frac{V}{M_{\rm Pl}^4}\left(\frac{k}{k_0}\right)^{n_{\rm T}}$$

Tensor spectral index: $n_{\rm T} = -2\epsilon$

- **Tensor-to-scalar ratio**

$$r = \frac{\mathcal{P}_{\rm T}}{\mathcal{P}_\zeta} = 16\epsilon$$

- **Consistency relation** (valid for *all* single field slow-roll inflation, easily generalizable to non-canonical kinetic term)

$$r = -8n_T$$

Planck 2015 constraints on inflation models

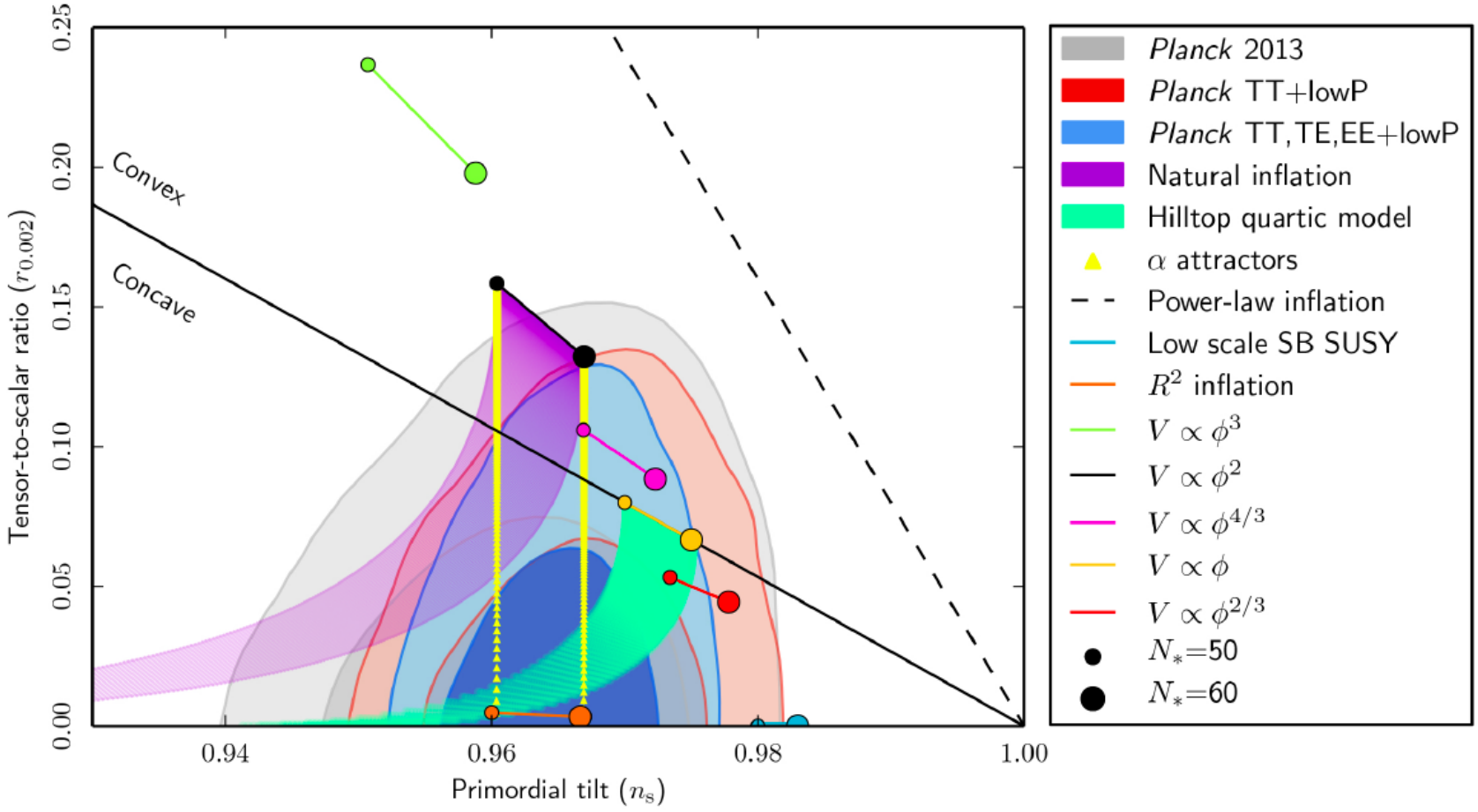

Marginalized joint 68% and 95% CL regions for n_s and $r_{0.002}$ from Planck in combination with other datasets, vs. theoretical prediction of selected inflation models.

PNG probes physics of the Early Universe

- PNG amplitude and shape measures deviations from standard inflation, perturbation generating processes after inflation, initial state before inflation, ...
- Inflation models which would yield the same predictions for scalar spectral index and tensor-to-scalar ratio might be distinguishable in terms of NG features.
- We should aim at "reconstructing" the inflationary action, starting from measurements of a few observables (like n_S, r, n_T, f_{NL}, g_{NL}, etc. …), just like in the nineties we were aiming at a reconstruction of the inflationary potential (see e.g. revival of the latter industry after the Bicep2 claim of PGW detection, ...).

Late nineties: simple-minded NG model

Many primordial (inflationary) models of non-Gaussianity can be represented in configuration space by the simple formula (Salopek & Bond 1990; Gangui et al. 1994; Verde et al. 1999; Komatsu & Spergel 2001)

$$\Phi = \phi_L + f_{NL} * (\phi_L^2 - \langle \phi_L^2 \rangle) + g_{NL} * (\phi_L^3 - \langle \phi_L^2 \rangle \phi_L) + \dots$$

where Φ is the large-scale gravitational potential (more precisely $\Phi = 3/5\ \zeta$ on superhorizon scales, where ζ is the gauge-invariant comoving curvature perturbation), ϕ_L its linear Gaussian contribution and f_{NL} the dimensionless *non-linearity parameter* (or more generally *non-linearity function*). The percent of non-Gaussianity in CMB data implied by this model is

NG % ~ 10^{-5} $|f_{NL}|$

~ 10^{-10} $|g_{NL}|$

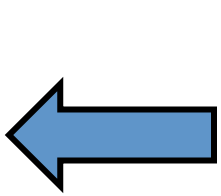

$< 10^{-5}$ from CMB & LSS

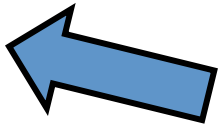

$< 10^{-5}$ from CMB & LSS

"non-Gaussian = non-dog"
(Ya.B. Zel'dovich)

Bispectrum & primordial non-Gaussianity

- Primordial NG probed fundamental physics during inflation, being sensitive to the ***interactions*** of fields present during inflation (different inflationary models predict different ***amplitudes and shapes*** of the bispectrum)

- Standard models of slow-roll inflation predict a ***tiny deviation from Gaussianity*** (Salopek & Bond ‘90; Gangui, Lucchin, Matarrese & Mollerach 1995; Acquaviva, Bartolo, Matarrese & Riotto 2003; Maldacena 2003)

2013 and 2015 *Planck* results ***consistent with such a prediction.***

- Searching for deviations from this *standard paradigm* is interesting *per-se* for theoretically well-motivated models of inflation and, as shown in *Planck 2013 results, can* ***severely limit*** various classes of inflationary models beyond the simplest paradigm. PNG probes interactions among particles at inflation energy scales. See recent literature on probing string-theory via oscillatory PNG (Arkani-Hamed & Maldacena 2015 “Cosmological collider physics”; Silverstein 2017 “The dangerous irrelevance of string theory”).

NG requires higher-order statistics (than the power-spectrum)

- The simplest statistics (but not fully general) measuring NG is the 3-point function or its Fourier transform, the "bispectrum":

$$\langle\phi(\mathbf{k}_1)\phi(\mathbf{k}_2)\phi(\mathbf{k}_3)\rangle = (2\pi)^3\delta^{(3)}(\mathbf{k}_1+\mathbf{k}_2+\mathbf{k}_3)\, B_\phi(k_1,k_2,k_3)$$

which carries shape information.

- In our simple linear + quadratic model above, the bispectrum of the gravitational potential reads:

$$B_\phi(k_1,k_2,k_3) = 2f_{NL}\,[P_\phi(k_1)P_\phi(k_2) + \text{cyclic terms}]$$

(by direct application of Wick's theorem), where

$$\langle\phi(\mathbf{k}_1)\phi(\mathbf{k}_2)\rangle = (2\pi)^3\delta^{(3)}(\mathbf{k}_1+\mathbf{k}_2)\, P_\phi(k_1)$$

Here the field φ is related to the comoving curvature perturbation ζ on super-Hubble scales by $\varphi = (3/5)\,\zeta$, and on super-Hubbler scales it reduces to Bardeen's gauge-invariant gravitational potential.

Bispectrum shape function

We can define the shape-function (f_{NL}=1) $S(k_1,k_2,k_3) \equiv \frac{1}{N}(k_1k_2k_3)^2 B_\Phi(k_1,k_2,k_3)$, where N is a suitable normalization.

In the scale-invariant case, the PS of the primordial gravitational potential takes the simple form $P_\Phi(k) = \Delta_\Phi k^{-3}$, hence:

$$
\begin{aligned}
&B_\Phi(k_1,k_2,k_3) \\
&\quad = 2f_{\rm NL}[P_\Phi(k_1)P_\Phi(k_2) + P_\Phi(k_2)P_\Phi(k_3) + P_\Phi(k_3)P_\Phi(k_1)] \\
&\quad \simeq 2f_{\rm NL}\frac{\Delta_\Phi^2}{(k_1k_2k_3)^2}\left(\frac{k_1^2}{k_2k_3} + \frac{k_2^2}{k_1k_3} + \frac{k_3^2}{k_1k_2}\right).
\end{aligned}
$$

For constant f_{NL} ("local" PNG) this implies

$$
S^{\rm local}(k_1,k_2,k_3) = \frac{1}{3}\left(\frac{k_1^2}{k_2k_3} + \frac{k_2^2}{k_1k_3} + \frac{k_3^2}{k_1k_2}\right).
$$

NOTE: The local shape is peaked on squeezed configurations, where one wave-number is much smaller than the other two.

Bispectrum shape function

- Another standard template shape is the "equilateral" one

$$S^{\rm equil}(k_1,k_2,k_3) = \frac{(k_1+k_2-k_3)(k_2+k_3-k_1)(k_3+k_1-k_2)}{k_1k_2k_3}$$

equilateral

local

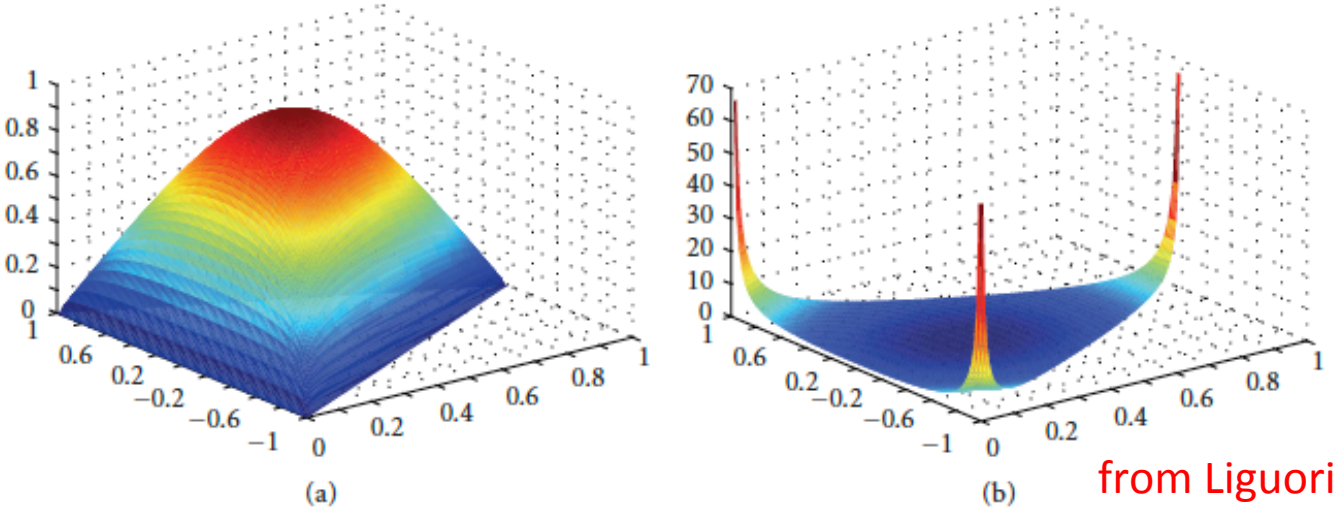

from Liguori et al. 2010

FIGURE 3: Shape functions for the scale-invariant equilateral (a) and local (b) models: $S(k_1,k_2,k_3) = S(\tilde{\alpha},\tilde{\beta})$ on transverse slices with $2\tilde{k} = k_1+k_2+k_3 = \text{const}$. See main text for the definition of the coordinate reparametrization in terms of $\tilde{\alpha}$ (y-axis) and $\tilde{\beta}$ (x-axis).

Where does NG come from (in standard inflation)?

- *Falk et al. (1993)* found $f_{NL} \sim \xi \sim \varepsilon^2$ (from non-linearity in the inflaton potential in a fixed de Sitter space) in the standard single-field slow-roll scenario

- *Gangui et al. (1994)*, using stochastic inflation found $f_{NL} \sim \varepsilon, \eta$ (from second-order gravitational corrections during inflation). *Acquaviva et al. (2003)* and *Maldacena (2003)* confirmed this estimate (up to numerical factors and momentum-dependent terms) with a full second-order approach. Weinberg extended the calculation of the bispectrum to 1-loop. One of these terms gives rise to the so-called "consistency relation", according to which found $f_{NL} = - 5/12(n_s-1)$ It has been shown that this term can be gauged away by a non-linear rescaling of coordinates, up to sub-leading terms. Hence the only residual term is proportional to ε i.e. to the amplitude of tensor modes. See however comments on this point, later on.

Bispectrum of a self-interacting scalar field in de Sitter space

Consider a scalar field χ with cubic self-interactions, i.e. with a term $\lambda\chi^3/3!$ In the Lagrangian. Call $\delta\chi$ the fluctuations around its v.e.v.. Its two and three-point functions in Fourier space (Falk et al. 1993; Gangui et al. 1994; Bernardeau et al. 2004), after the rescaling $\delta\chi = \widetilde{\delta\chi}/a$ read:

$$\langle 0|\widetilde{\delta\chi}(\tau,\mathbf{k})\widetilde{\delta\chi}(\tau',\mathbf{k}')|0\rangle = \delta^{(3)}(\mathbf{k}+\mathbf{k}')G(k,\tau,\tau')$$

$$\langle \widetilde{\delta\chi}_{\mathbf{k}_1}\widetilde{\delta\chi}_{\mathbf{k}_2}\widetilde{\delta\chi}_{\mathbf{k}_3}\rangle = -\mathrm{i}\lambda\delta^{(3)}(\mathbf{k_1}+\mathbf{k_2}+\mathbf{k}_3)\int_{-\infty}^{\tau}\frac{-\mathrm{d}\tau'}{H\tau'}[G(k_1,\tau,\tau')G(k_2,\tau,\tau')G(k_3,\tau,\tau') - G^*(k_1,\tau,\tau')G^*(k_2,\tau,\tau')G^*(k_3,\tau,\tau')]\ .$$

where the Green's function reads

$$G(k,\tau,\tau') = \frac{1}{2k}\left(1-\frac{\mathrm{i}}{k\tau}\right)\left(1+\frac{\mathrm{i}}{k\tau'}\right)\exp[\mathrm{i}k(\tau'-\tau)]$$

The bispectrum is (ζ being a function of order 1)

$$\langle \delta\chi_{\mathbf{k}_1}\delta\chi_{\mathbf{k}_2}\delta\chi_{\mathbf{k}_3}\rangle = v_3(k_i)\sum_i\prod_{J\neq i}\frac{H^2}{2k_j^3} \qquad v_3(k_i) = \frac{\lambda}{3H^2}\left[\gamma+\zeta(k_i)+\log[-k_T\tau]\right]$$

Bispectrum of standard inflation

In the case of standard slow-roll single-field inflation one finds (Acquaviva et al. 2003; Maldacena 2003) the simple shape

$$
\begin{aligned}
&S^{\mathrm{Mald}}(k_1,k_2,k_3)\\
&\quad\propto (3\epsilon-2\eta)\left[\frac{k_1^2}{k_2k_3}+\frac{k_2^2}{k_1k_3}+\frac{k_3^2}{k_1k_2}\right]\\
&\qquad+\epsilon\left[(k_1k_2^2+5\,\mathrm{perm.})+4\frac{k_1^2k_2^2+k_2^2k_3^2+k_3^2k_1^2}{k_1k_2k_3}\right]\\
&\quad\simeq (6\epsilon-2\eta)S^{\mathrm{local}}(k_1,k_2,k_3)+\frac{5}{3}\epsilon\,S^{\mathrm{equil}}(k_1,k_2,k_3
\end{aligned}
$$

where the factor in front of the local shape is proportional to the tilt n_S-1. But … is it observable?

Single-field Inflation bispectra

$$\left\langle \zeta_{\vec{k}_1} \zeta_{\vec{k}_2} \zeta_{\vec{k}_3} \right\rangle = \frac{H^4}{M_{pl}^4} \frac{1}{\epsilon} \delta^3 \left(\sum \vec{k}_i \right) \mathcal{M}_1$$

$$\left\langle \zeta_{\vec{k}_1} \zeta_{\vec{k}_2} h_{\vec{k}_3} \right\rangle = \frac{H^4}{M_{pl}^4} \frac{1}{\epsilon} \delta^3 \left(\sum \vec{k}_i \right) \mathcal{M}_2$$

$$\left\langle \zeta_{\vec{k}_1} \gamma_{\vec{k}_2} \gamma_{\vec{k}_3} \right\rangle = \frac{H^4}{M_{pl}^4} \delta^3 \left(\sum \vec{k}_i \right) \mathcal{M}_3$$

$$\left\langle \gamma_{\vec{k}_1} \gamma_{\vec{k}_2} \gamma_{\vec{k}_3} \right\rangle = \frac{H^4}{M_{pl}^4} \delta^3 \left(\sum \vec{k}_i \right) \mathcal{M}_4$$

Maldacena 2003

Separability

The above shapes share the important property of being separable, i.e.

$$S(k_1, k_2, k_3) = X(k_1)Y(k_2)Z(k_3) + 5\,\text{perms},$$

This important property greatly simplifies the calculation of the bispectrum.

there are more shapes of non-Gaussianity from inflation than ... stars in the sky

Starting point: the curvature (gravitational potential) bispectrum

Bispectrum of primordial curvature perturbations

Amplitude

Shape

$$\langle \Phi(\vec{k}_1)\Phi(\vec{k}_2)\Phi(\vec{k}_3)\rangle = (2\pi)^3\delta^{(3)}(\vec{k}_1+\vec{k}_2+\vec{k}_3) f_{\rm NL} F(k_1,k_2,k_3)$$

Local NG

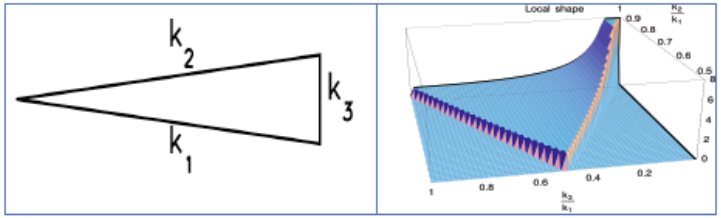

Multi-field models of inflation;
Cuvaton models;
Ekpyrotic/cyclic models

Equilateral NG

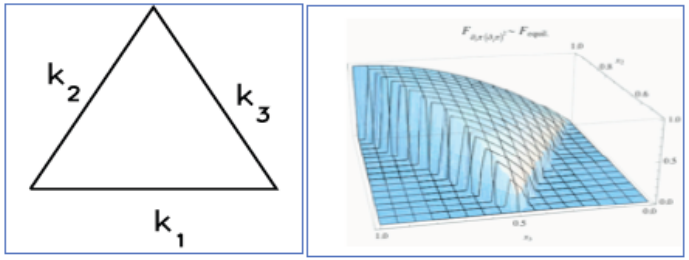

Single inflaton with non-standard kinetic term;
higher derivative interactions

Orthogonal NG

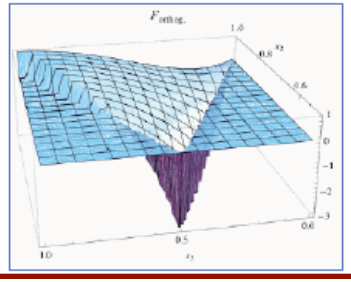

Single inflaton with non-standard kinetic term;
higher derivative interactions

Also: directionally dependent bispectra,
tensor bispectra and many others.

Models behind bispectrum shapes (... a few of them)

- **local** shape: Multi-field models, Curvaton, Ekpyrotic/cyclic, etc. ...
- **equilateral** shape: Non-canonical kinetic term, DBI, K-inflation, Higher-derivative terms, Ghost, EFT approach
- **orthogonal** shape: Distinguishes between variants of non-canonical kinetic term, higher-derivative interactions, Galilean inflation
- **flattened** shape: non-Bunch-Davies initial state and higher-derivative interactions, models where a Galilean symmetry is imposed. The flat shape can be written in terms of equilateral and orthogonal.

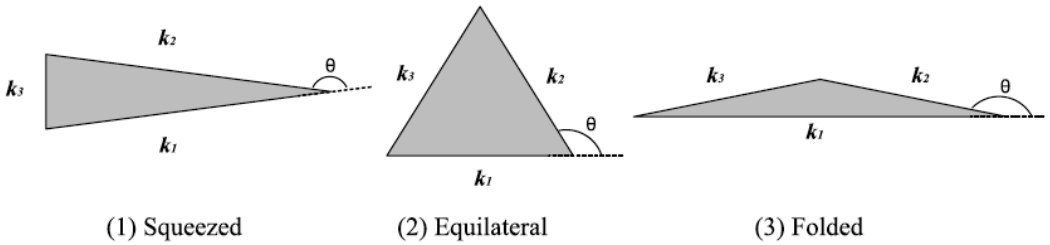

(1) Squeezed (2) Equilateral (3) Folded

NG shapes: local

Bispectrum peaks for squeezed triangles $k_1 \ll k_2 \sim k_3$

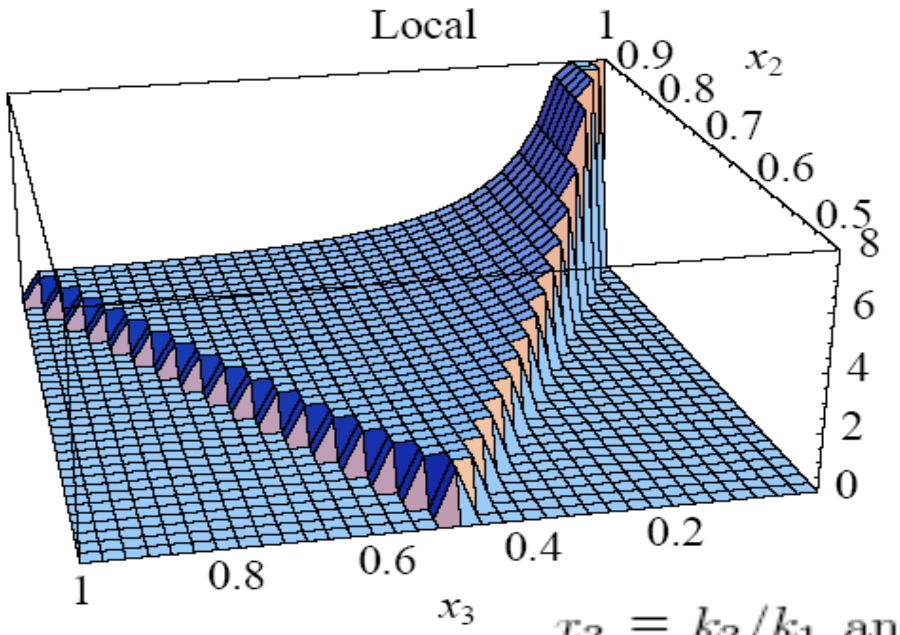

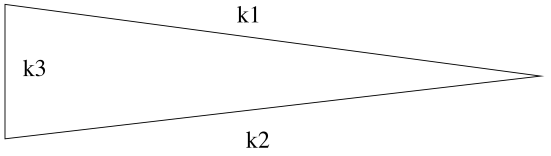

$$F(1,x_2,x_3)x_2^2x_3^2$$

$x_3 \equiv k_3/k_1$ and $x_2 \equiv k_2/k_1$

Babich et al. astro-ph/0405356

$$\Phi(\mathbf{x}) = \Phi_L(\mathbf{x}) + f_{\rm NL}\Phi_L^2(\mathbf{x})$$

Non-linearities develop outside the horizon during or immediately after inflation (e.g. multifield models of inflation)

NG shapes: equilateral

Bispectrum peaks for equilateral triangles: $k_1=k_2=k_3$

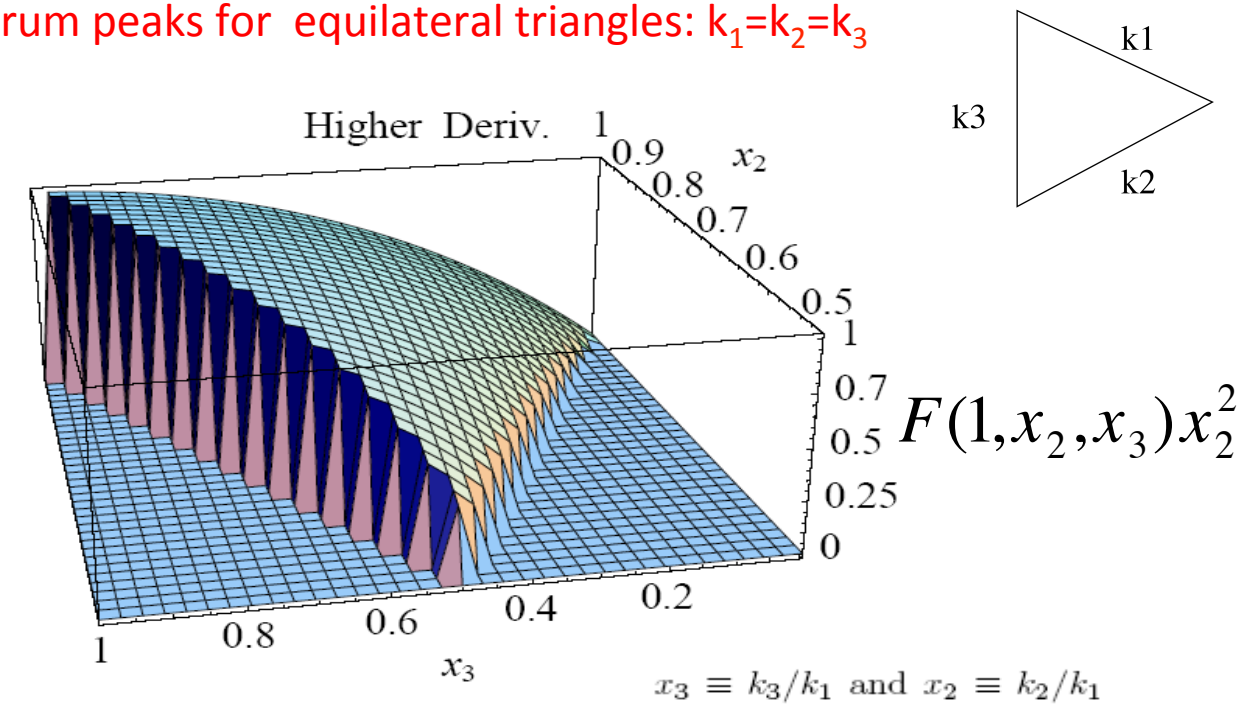

Babich et al. (2004)

Single field models of inflation with non-canonical kinetic term L=P(φ, X) where X=(∂ φ)^2 (DBI or K-inflation) where NG comes from higher derivative interactions of the inflaton field

Example: $\dot{\delta\phi}(\nabla\delta\phi)^2$

NG shapes: flattened

Bispectrum peaks for flattened triangles $k_2 = k_1 + k_3$

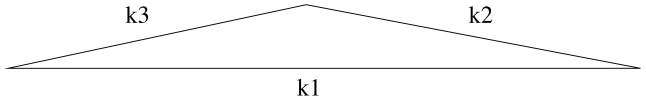

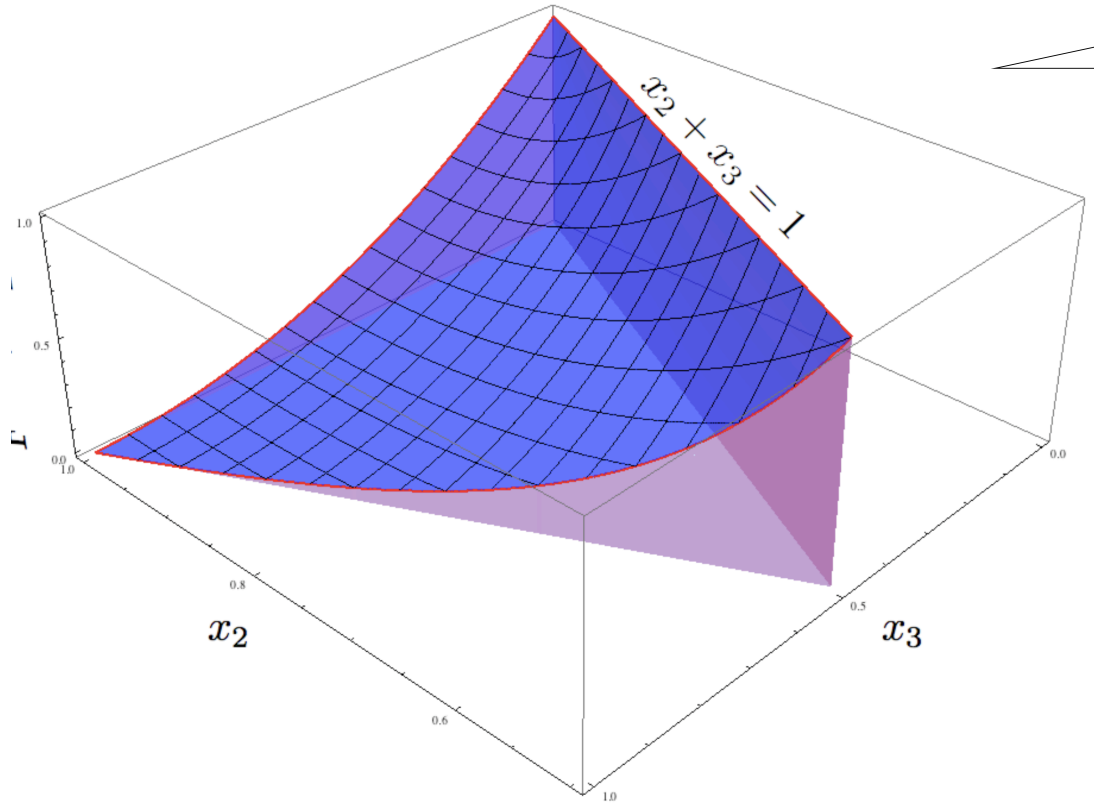

(typical of NG from excited initial states, see Meerburg et al. arXiv:0901.4044; Chen et al. hep-th/0605045; Holman & Tolley arXiv:0710.1302; or from higher derivative interactions, Fasiello, Bartolo, Matarrese, Riotto arXiv:1004.0893)

Warning: this is not a blind search for NG

- Detecting a non-zero primordial bispectrum (e.g. non-zero f_{NL}) proves that the initial seeds were non-Gaussian. Similarly for the trispectrum, etc. …

- Not detecting non-zero f_{NL} however, doesn't prove Gaussianity!

- There are infinitely many ways PNG can evade observational bounds optimized to search for f_{NL} and similar higher-order parameters

A worked example (Scherrer & Schaefer 1995)

- Assume the linear density contrast δ is non-Gaussian.
- By the central limit theorem, the gravitational potential ϕ (which yields large-scale CMB anisotropies) tends to be much more Gaussian. Indeed, by solving Poisson's equation,

$$\phi(\mathbf{r}) = -Ga^2\bar{\rho}\int \frac{\delta(\mathbf{r}')d^3\mathbf{r}'}{|\mathbf{r}-\mathbf{r}'|}\,.$$

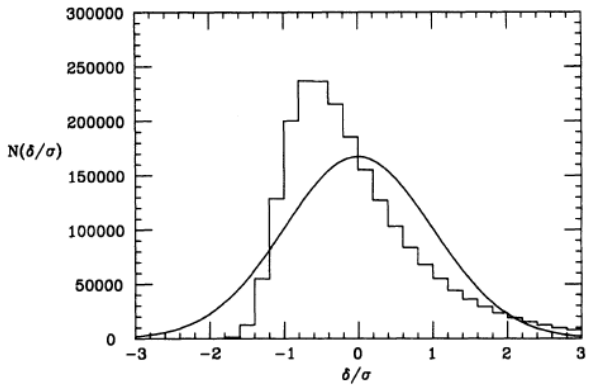

FIG. 1a

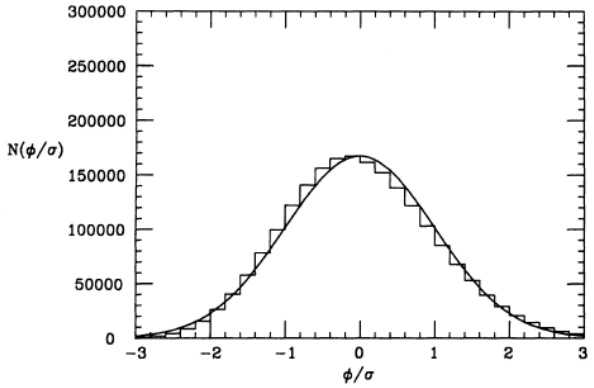

FIG. 1b

FIG. 1.—(*a*) The distribution of densities in the model given by the Wold representation: $\delta(\mathbf{r}) = \int f(|\mathbf{r}-\mathbf{r}'|)\Delta(\mathbf{r}')d^3\mathbf{r}'$, where $\Delta(\mathbf{r})$ is an uncorrelated field with a gamma distribution, and f is chosen to give a Zel'dovich power spectrum [$P(k) \propto k$] for the density field. Solid curve is a Gaussian distribution with the same mean and variance. (*b*) The distribution of potentials for the same model. Solid curve is a Gaussian distribution with the same mean and variance.

Inflation in the scaling limit

(Matarrese, Ortolan & Lucchin 1989)

$$\dot{\phi} = -\frac{1}{3H(\phi)}\frac{\partial V(\phi)}{\partial \phi} + \frac{H^{3/2}(\phi)}{\sigma^{1/2}}\eta(t) \ ,$$

where $H(\phi) = \sqrt{V/3\sigma^2}$ and $\sigma \equiv 1/\sqrt{8\pi G}$

$$\langle \eta(t) \rangle = 0 \ ,$$

$$\langle \eta(t)\eta(t') \rangle = 2\epsilon\delta(t-t'), \quad \epsilon \approx \hbar\sigma/8\pi^2$$

Multiplicative stochastic process

$$\mathcal{P}(\phi, t) = \langle \delta(\phi - \phi[\eta(t)]) \rangle_\eta$$

NG is generic in the late-time "scaling limit"

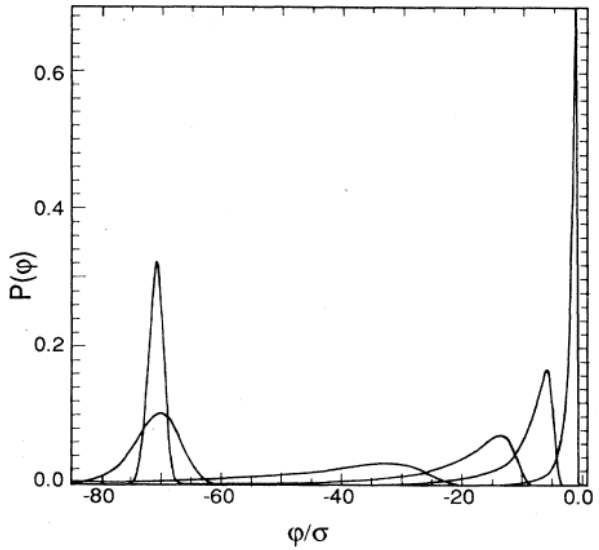

FIG. 2. The distribution for the inflaton with quartic potential is plotted at different times. From left to right: $\tau/\tau_{sc}=10^{-3}$, 10^{-2}, 1.28, 1.492, 1.499, and 1.5. The parameters are $\lambda=10^{-4}$, $H_*/\sigma\simeq 14.5$.

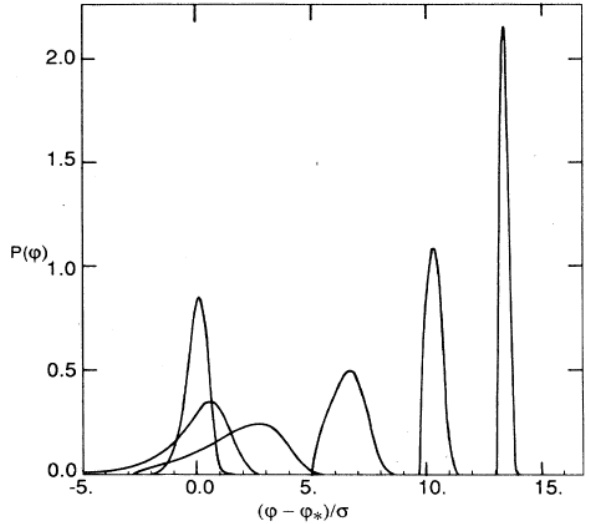

FIG. 3. The distribution for the inflaton with exponential potential is plotted at different times. From left to right: $\tau/\tau_{sc}=10^{-2}$, 8×10^{-2}, 8×10^{-1}, 3, 5, and 7. The parameters are $\lambda=0.5$, $H_*/\sigma\simeq 14.5$.

NG is generic in the late-time "scaling limit"

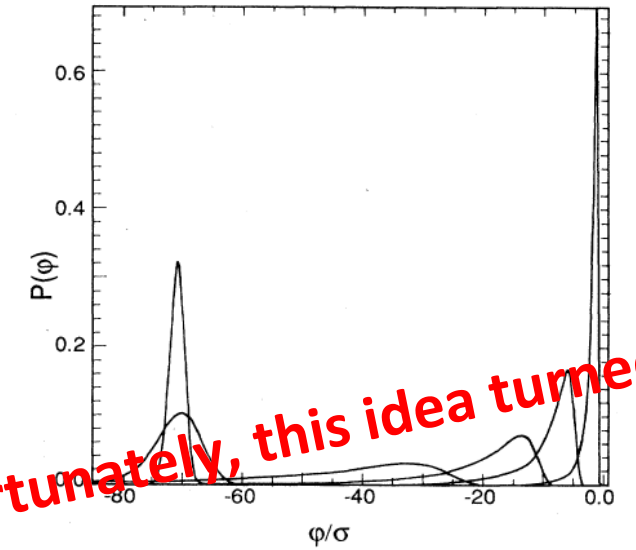

FIG. 2. The distribution for the inflaton with quartic potential is plotted at different times. From left to right: $\tau/\tau_{sc}=10^{-3}$, 10^{-2}, 1.28, 1.492, 1.499, and 1.5. The parameters are $\lambda=10^{-4}$, $H_*/\sigma\simeq 14.5$.

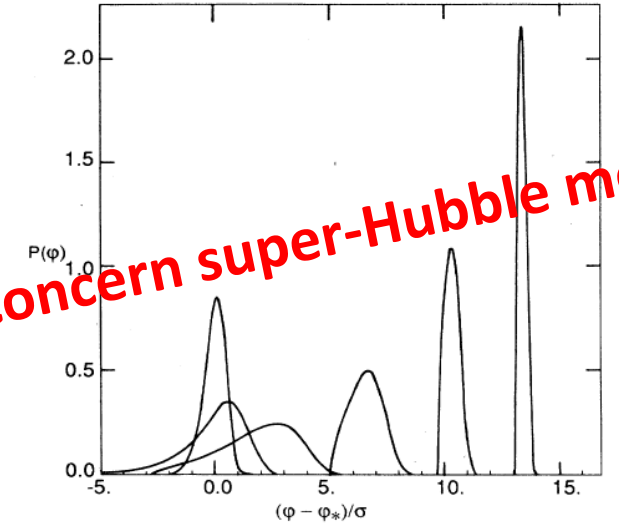

FIG. 3. The distribution for the inflaton with exponential potential is plotted at different times. From left to right: $\tau/\tau_{sc}=10^{-2}$, 8×10^{-2}, 8×10^{-1}, 3, 5, and 7. The parameters are $\lambda=0.5$, $H_*/\sigma\simeq 14.5$.

Unfortunately, this idea turned out to concern super-Hubble modes!!

Why is this NG dynamics not difrectly affecting observable perturbation modes?

- This NG dynamics has to do with fluctuations w.r.t. the global, i.e. super-horizon, average; observable fluctuations instead have to be computed on top of the local mean (i.e. w.r.t to our Hubble volume). See Salopek, Bond & Bardeen 1989; Kofman et al. 1991
- If the underlying noise is “white”, because of the Markov property, any cross-talk between super-Hubble and sub-Hubble modes disappears and observable fluctuations become nearly Gaussian. See: Mollerach, Matarrese, Ortolan & Lucchin 1991
- Is this really the final word?
- The noise is not really white: colored noise leads to cross-talk and potentially observable effects (Matarrese, Musso & Riotto 2004)
- The super-Hubble dynamics can be related to the so-called NG landscape (Nurmi et al. 2013; LoVerde et al. 2013).
- Potentially interesting consequences (e.g. intermittency) yet to be explored …

Non-Gaussianity &
Cosmic Microwave Background (CMB)

The scientific results that we present today are a product of the Planck Collaboration, including individuals from more than 100 scientific institutes in Europe, the USA and Canada

Planck is a project of the European Space Agency, with instruments provided by two scientific Consortia funded by ESA member states (in particular the lead countries: France and Italy) with contributions from NASA (USA), and telescope reflectors provided in a collaboration between ESA and a scientific Consortium led and funded by Denmark.

NG CMB simulated maps

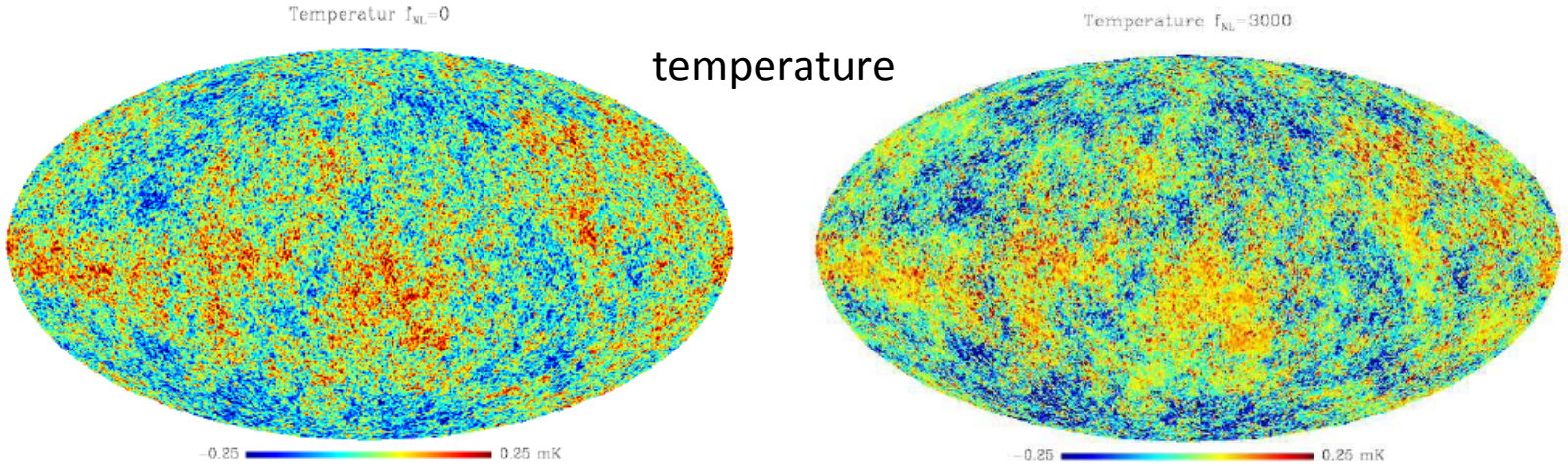

temperature

Gaussian

Liguori, Yadav, Hansen, Komatsu, Matarrese & Wandelt 2007

non-Gaussian

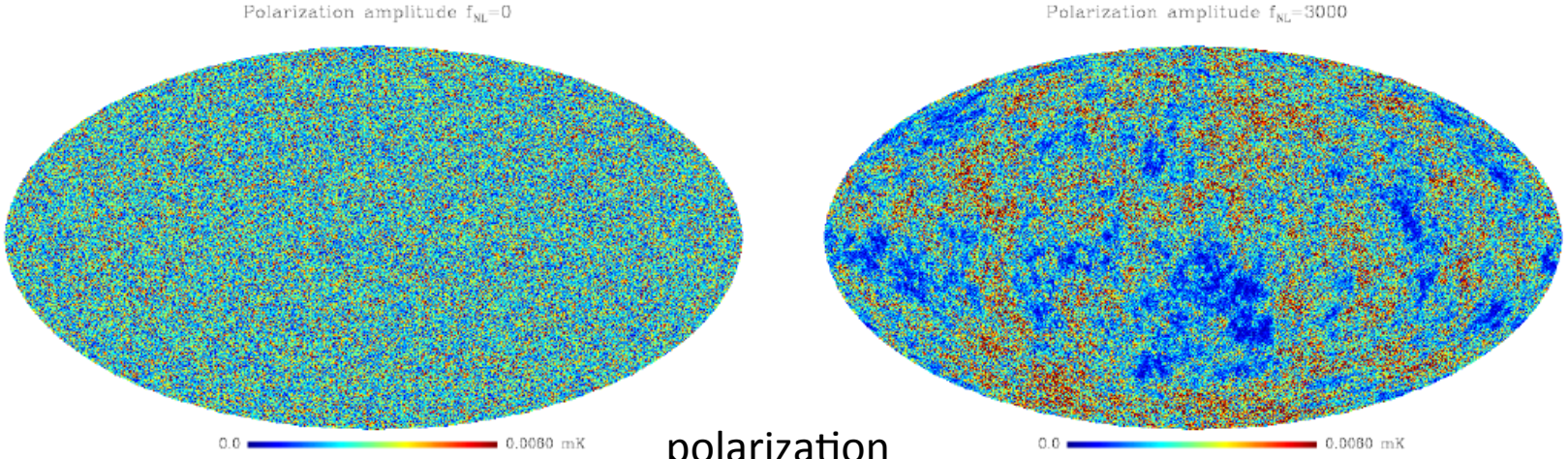

polarization

Planck 2015 results XVII: *Planck* collaboration: A&A 594, A17 (2016)

- Constrain (with high precision) and/or detect primordial non-Gaussianity (NG) as due to (non-standard) inflation (NG amplitude and shape measure deviations from standard inflation, perturbation generating processes after inflation, initial state before inflation, ...)

- We test: ***local, equilateral, orthogonal*** shapes (+ many more) for the bispectrum and constrain primordial trispectrum parameter g_{NL} (τ_{NL} constrained in previous release).

- Currently we are working at a final, *Planck* legacy release, which will improve the 2015 results in terms of more refined treatment of E-mode polarization (including lower and higher l.

CMB bispectrum representation

$$B^{m_1 m_2 m_3}_{\ell_1 \ell_2 \ell_3} \equiv \langle a_{\ell_1 m_1} a_{\ell_2 m_2} a_{\ell_3 m_3} \rangle$$

$$= \mathcal{G}^{\ell_1 \ell_2 \ell_3}_{m_1 m_2 m_3} \, b_{\ell_1 \ell_2 \ell_3}$$

Gaunt integrals

$$\mathcal{G}^{\ell_1 \ell_2 \ell_3}_{m_1 m_2 m_3} \equiv \int Y_{\ell_1 m_1}(\hat{\boldsymbol{n}}) \, Y_{\ell_2 m_2}(\hat{\boldsymbol{n}}) \, Y_{\ell_3 m_3}(\hat{\boldsymbol{n}}) \, d^2\hat{\boldsymbol{n}}$$

$$= h_{\ell_1 \ell_2 \ell_3} \begin{pmatrix} \ell_1 & \ell_2 & \ell_3 \\ m_1 & m_2 & m_3 \end{pmatrix},$$

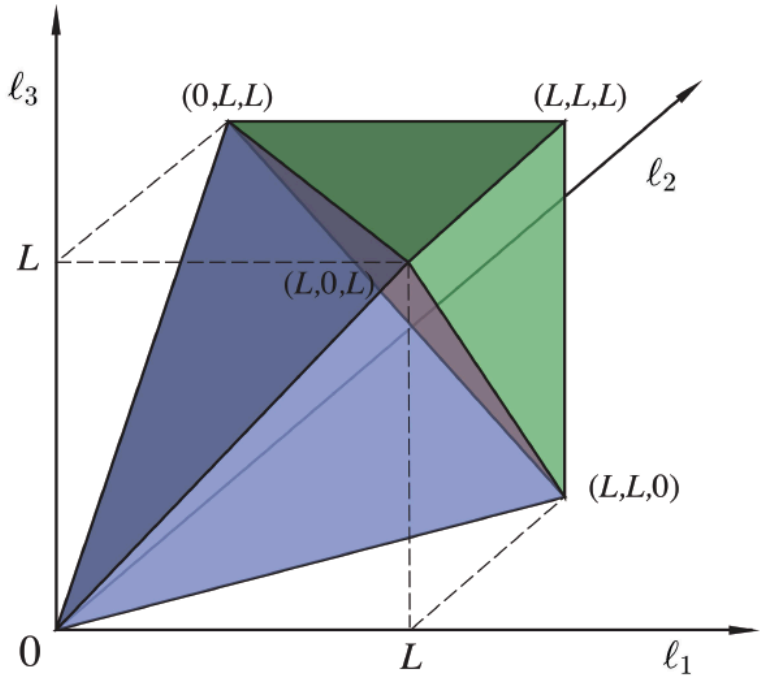

Triangle condition: $\ell_1 \le \ell_2 + \ell_3$ for $\ell_1 \ge \ell_2, \ell_3$, +perms.

Parity condition: $\ell_1 + \ell_2 + \ell_3 = 2n, \quad n \in \mathbb{N},$

Resolution: $\ell_1, \ell_2, \ell_3 \le \ell_{\max}, \quad \ell_1, \ell_2, \ell_3 \in \mathbb{N}.$

Optimal f_{NL} bispectrum estimator

$$\hat{f}_{NL} = \frac{1}{N}\sum B^{m_1 m_2 m_3}_{\ell_1 \ell_2 \ell_3} \left(C^{-1}a\right)^{m_1}_{\ell_1} \left(C^{-1}a\right)^{m_2}_{\ell_2} \left(C^{-1}a\right)^{m_3}_{\ell_3} - 3C^{-1}_{\ell_1 m_1 \ell_2 m_2} \left(C^{-1}a\right)^{m_3}_{\ell_3}$$

Leaving aside complications coming from breaking of statistical isotropy (sky-cut, noise, …), one can see that we are extracting the 3-point function from the data and fitting theoretical bispectrum templates to it

$$\hat{f}_{NL} = \frac{1}{N}\sum_{\ell_i m_i} B^{m_1 m_2 m_3}_{\ell_1 \ell_2 \ell_3} \frac{a^{m_1}_{\ell_1}}{C_{\ell_1}} \frac{a^{m_2}_{\ell_2}}{C_{\ell_2}} \frac{a^{m_3}_{\ell_3}}{C_{\ell_3}}$$

A brute force implementation scales like $\ell^5_{\max}$. Unfeasible at Planck (or even WMAP) resolution.

Can achieve massive speed improvement ($\ell^3_{\max}$ scaling) if the reduced bispectrum is *separable* (KSW method: Komatsu, Spergel, Wandelt 2003).

$$b_{\ell_1 \ell_2 \ell_3} = \sum_{ijk} X^i_{\ell_1} Y^j_{\ell_2} Z^k_{\ell_3} \Rightarrow B^{m_1 m_2 m_3}_{\ell_1 \ell_2 \ell_3} = b_{\ell_1 \ell_2 \ell_3} \int Y^{m_1}_{\ell_1}(\Omega) Y^{m_2}_{\ell_2}(\Omega) Y^{m_3}_{\ell_3}(\Omega)$$

Optimal f_{NL} bispectrum estimator

$$\hat{f}_{NL} = \frac{1}{N} \sum B^{m_1 m_2 m_3}_{\ell_1 \ell_2 \ell_3} \left[\left(C^{-1}a\right)^{m_1}_{\ell_1} \left(C^{-1}a\right)^{m_2}_{\ell_2} \left(C^{-1}a\right)^{m_3}_{\ell_3} - 3C^{-1}_{\ell_1 m_1 \ell_2 m_2} \left(C^{-1}a\right)^{m_3}_{\ell_3} \right]$$

The theoretical template needs to be written in separable form. This can be done in different ways and *alternative implementations differ basically in terms of the separation technique adopted and of the projection domain*.

- KSW (Komatsu, Spergel & Wandelt 2003) separable template fitting + Skew-C_l extension (Munshi & Heavens 2010)
- Binned bispectrum (Bucher, Van Tent & Carvalho 2009)
- Modal expansion (Fergusson, Liguori & Shellard 2009)

Going beyond the standard approach

- in Verde, Jimenez, Alvarez-Gaume, Heavens & Matarrese 2013 we provided an exact expression for the multi-variate joint probability distribution function of non-Gaussian fields primordially arising from local transformations of a Gaussian field.
- We applied our expression to the non-Gaussianity estimation from CMB maps and the halo mass function where we obtain analytical expressions.
- We also provided analytic approximations and their range of validity. And for the CMB we gave a fast way to compute the PDF which is valid up to more than 7σ for f_{NL} values not ruled out by current observations, which consists of expressing the PDF as a combination of bispectrum and trispectrum of the temperature maps.
- The resulting expression is valid for any kind of non-Gaussianity and is not limited to the local type.

These results may serve as the basis for a fully Bayesian analysis of the non-Gaussianity parameter.

Going to higher order?

$$\mathcal{P}(a|f_{\rm NL}) = \frac{(\det C^{-1})^{1/2}}{(2\pi)^{n/2}} \exp\left[-\frac{1}{2}\sum_{\ell\ell' mm'} a_\ell^{*m}(C^{-1})_{\ell m\ell' m'} a_{\ell'}^{m'}\right] \times$$

$$\left\{1 + \frac{1}{6}\sum_{\text{all } \ell_i m_j} \langle a_{\ell_1}^{m_1} a_{\ell_2}^{m_2} a_{\ell_3}^{m_3}\rangle \left[(C^{-1}a)_{\ell_1}^{m_1}(C^{-1}a)_{\ell_2}^{m_2}(C^{-1}a)_{\ell_3}^{m_3} - 3(C^{-1})_{l_1,l_2}^{m_1 m_2}(C^{-1}a)_{l_3}^{m_3}\right] +\right.$$

$$\frac{1}{24}\sum_{\text{all } \ell m} \langle a_{\ell_1}^{m_1} a_{\ell_2}^{m_2} a_{\ell_3}^{m_3} a_{\ell_4}^{m_4}\rangle \left[3(C^{-1})_{\ell_1\ell_2}^{m_1 m_2}(C^{-1})_{\ell_3,\ell_4}^{m_3 m_4}\right.$$

$$\left. -6(C^{-1})_{\ell_1,\ell_2}^{m_1 m_2}(C^{-1}a)_{\ell_3}^{m_3}(C^{-1}a)_{\ell_4}^{m_4} + (C^{-1}a)_{\ell_1}^{m_1}(C^{-1}a)_{\ell_2}^{m_2}(C^{-1}a)_{\ell_3}^{m_3}(C^{-1}a)_{\ell_4}^{m_4}\right] +$$

$$\frac{1}{72}\sum_{l_1,\ldots,l_6} \langle a_{\ell_1}^{m_1} a_{\ell_2}^{m_2} a_{\ell_3}^{m_3}\rangle\langle a_{\ell_4}^{m_4} a_{\ell_5}^{m_5} a_{\ell_6}^{m_6}\rangle \left[(C^{-1}a)_{\ell_1}^{m_1}(C^{-1}a)_{\ell_2}^{m_2}(C^{-1}a)_{\ell_3}^{m_3}(C^{-1}a)_{\ell_4}^{m_4}(C^{-1}a)_{\ell_5}^{m_5}(C^{-1}a)_{\ell_6}^{m_6}\right.$$

$$-15(C^{-1})_{\ell_1\ell_2}^{m_1 m_2}(C^{-1}a)_{\ell_3}^{m_3}(C^{-1}a)_{\ell_4}^{m_4}(C^{-1}a)_{\ell_5}^{m_5}(C^{-1}a)_{\ell_6}^{m_6}$$

$$\left.\left. -15(C^{-1})_{\ell_1\ell_2}^{m_1 m_2}(C^{-1})_{\ell_3\ell_4}^{m_3 m_4}(C^{-1})_{\ell_5\ell_6}^{m_5 m_6} + 45(C^{-1})_{\ell_1\ell_2}^{m_1 m_2}(C^{-1})_{\ell_3\ell_4}^{m_3 m_4}(C^{-1}a)_{\ell_5}^{m_5}(C^{-1}a)_{\ell_6}^{m_6}\right]\right\}$$

It may become important if we want to detect NG in observables where f_{NL} is large (e.g. in high-redshift probes) and/or if both f_{NL} (→ leading order bispectrum) and g_{NL} (leading-order trispectrum) are both depending on the same underlying physical coupling constant that we aim at determining. **Note: The one above is a *contracted* form; more combinations in the general expression.**

Verde, Jimenez, Alvarez-Gaume, Heavens & Matarrese 2013

Bispectrum shapes (modal representation)

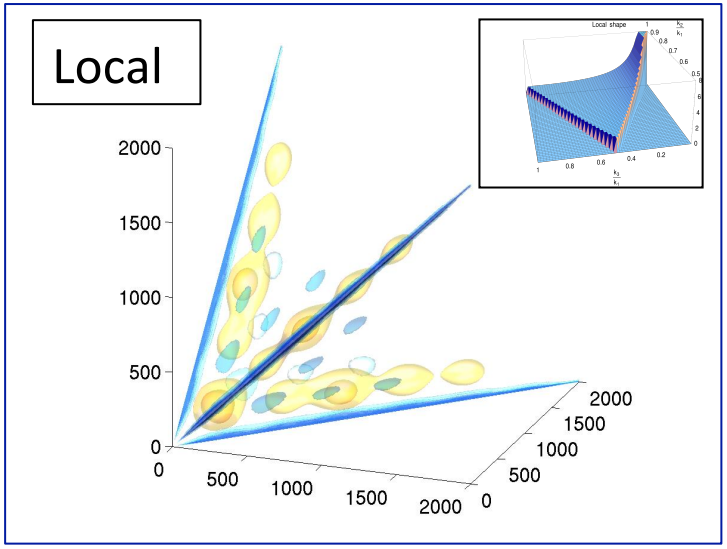

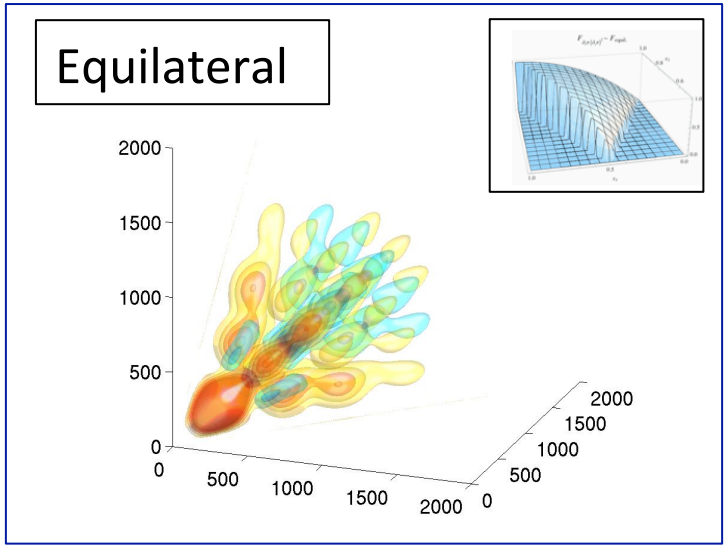

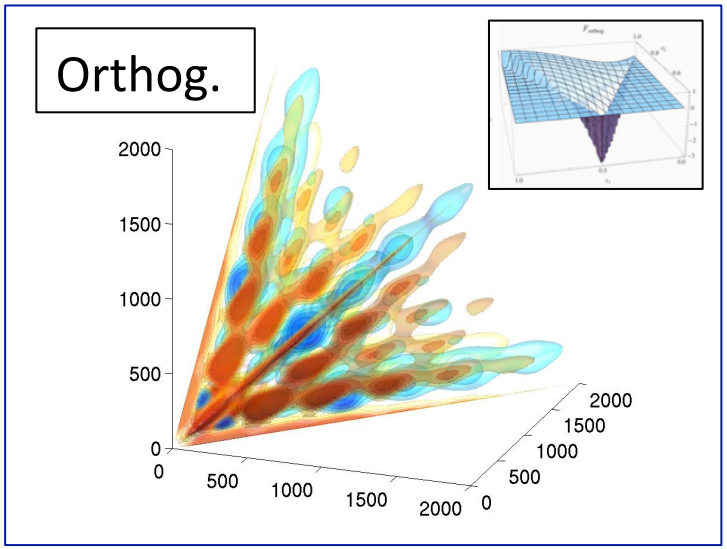

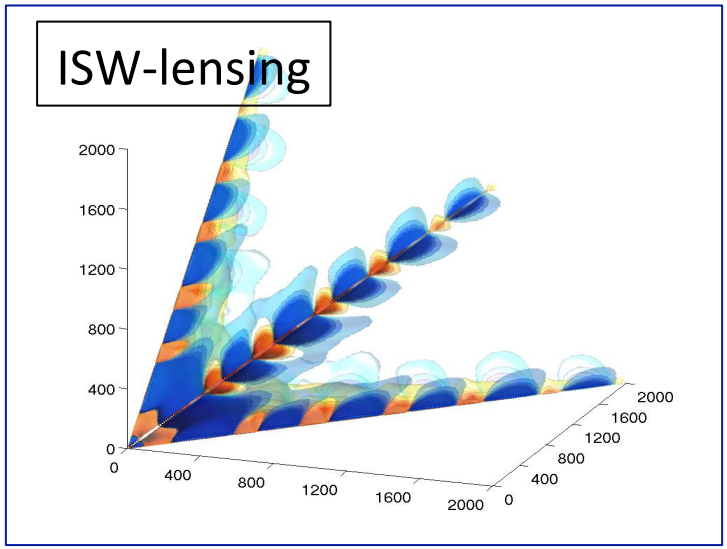

The 2015 *Planck* bispectrum (modal)

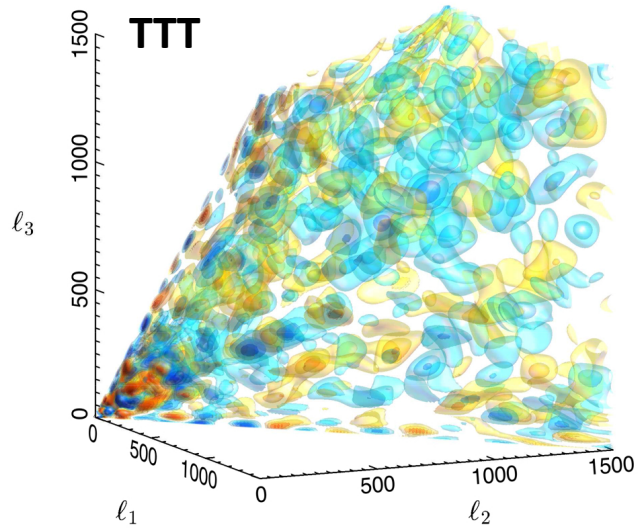

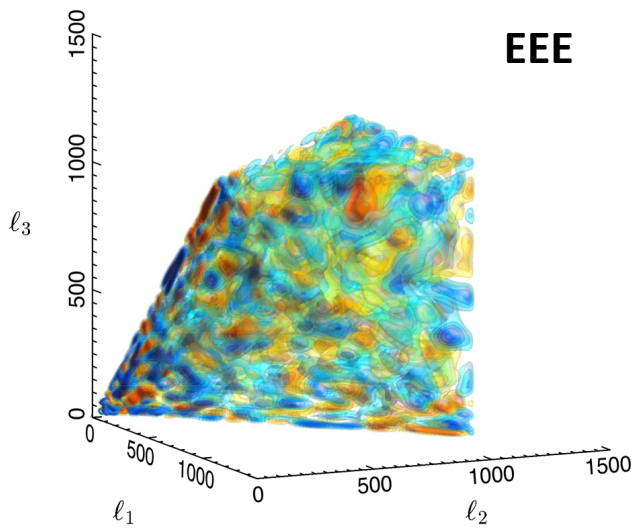

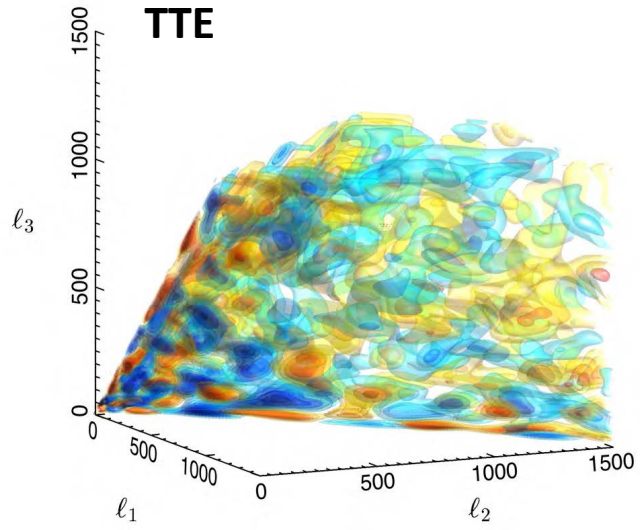

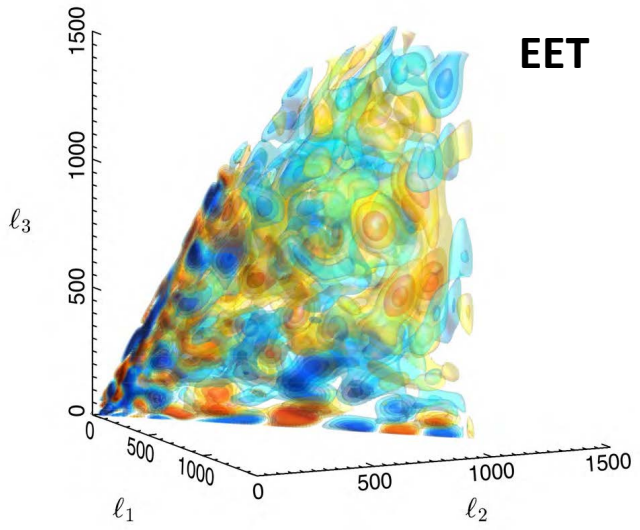

(S/N weighted)

Planck TTT: 2013 vs Planck 2015

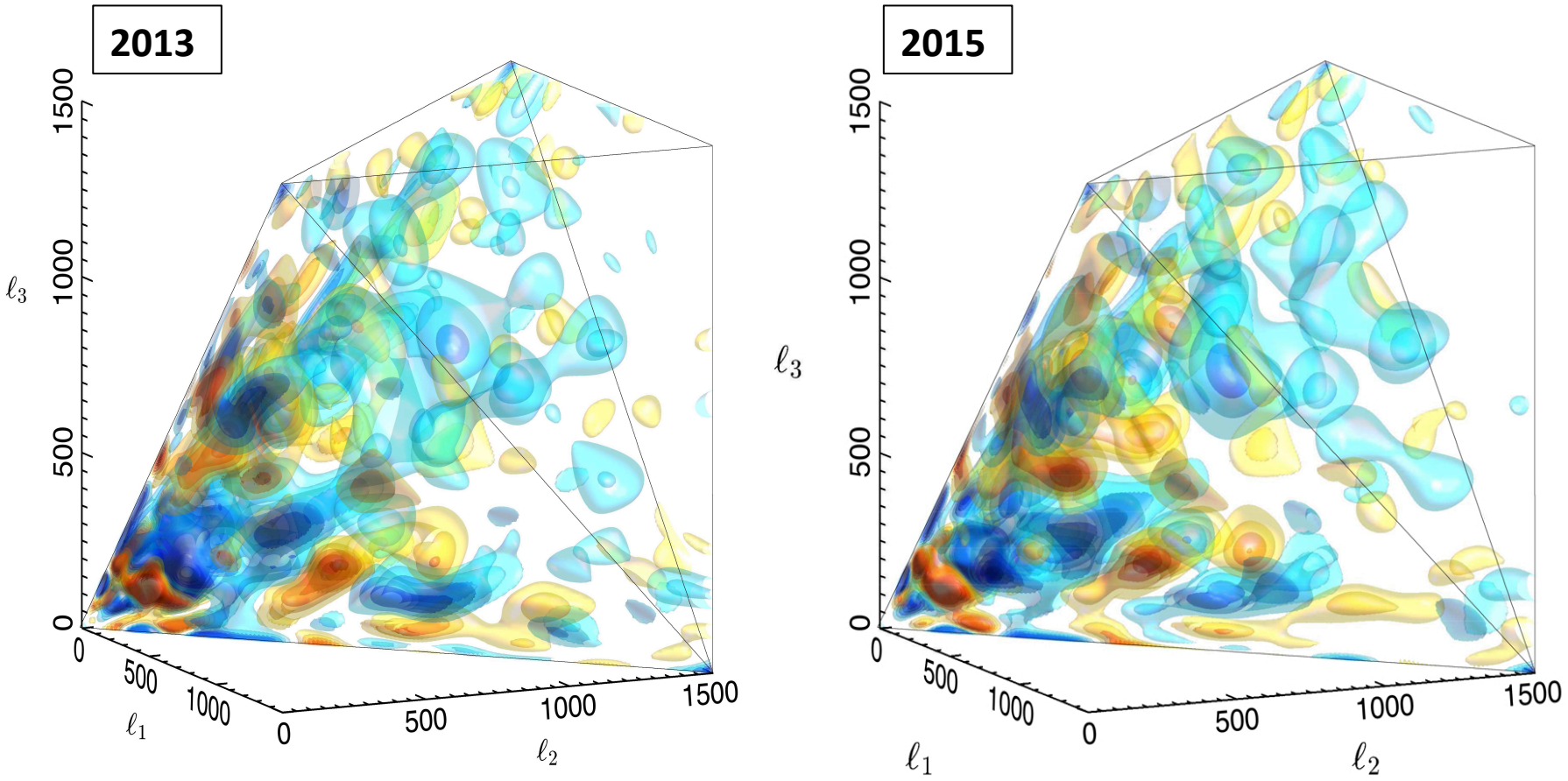

Primordial NG Planck results: Ade et al., Planck 2015 results. XVII

Method: modal bispectrum reconstruction (Fergusson, Liguori, Shellard 2010, 2011)

Planck TTT: 2013 vs Planck 2015

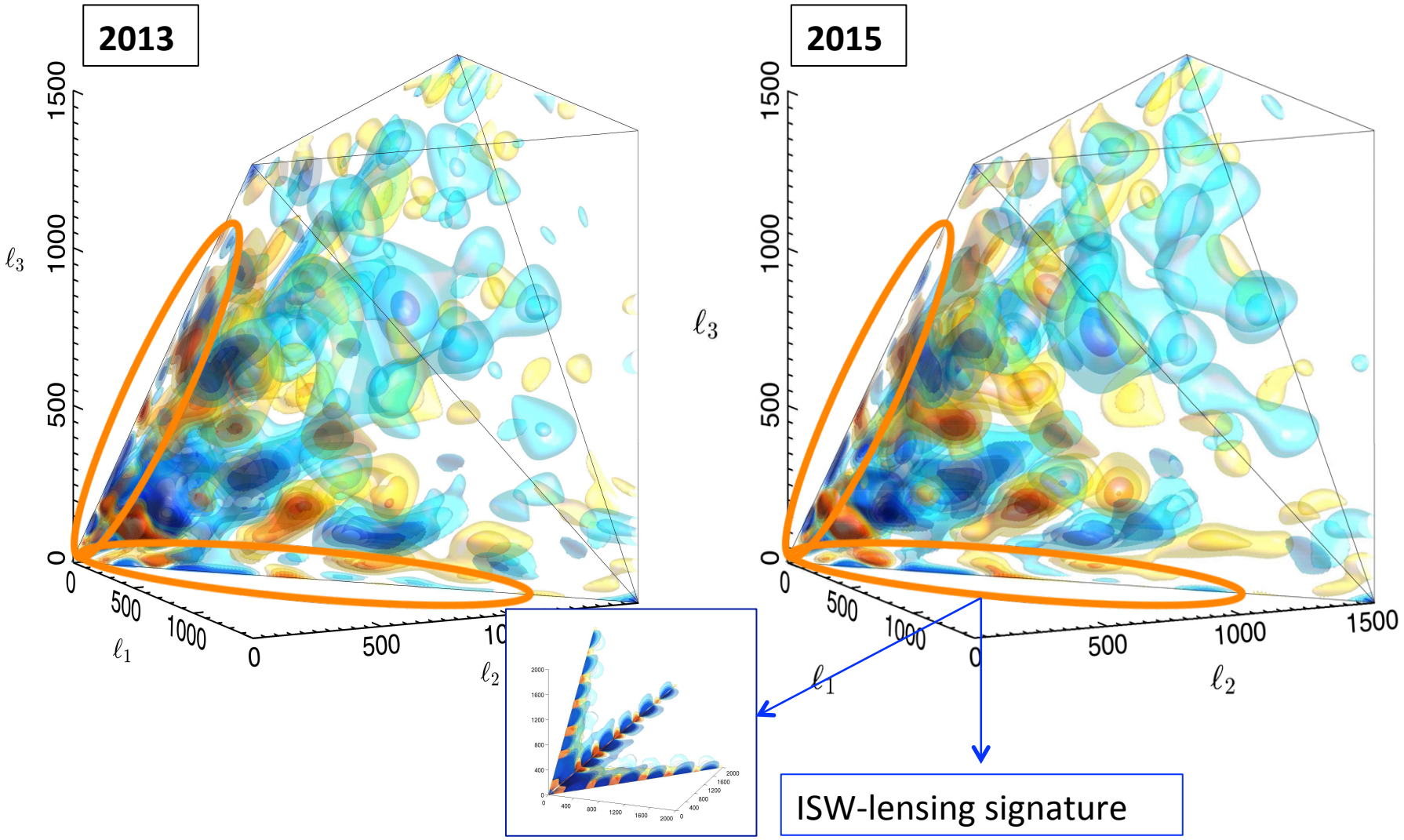

f_{NL} from *Planck* bispectrum (KSW)

Shape and method	f_{NL}(KSW) Independent	f_{NL}(KSW) ISW-lensing subtracted
SMICA (T)		
Local	10.2 ± 5.7	**2.5 ± 5.7**
Equilateral	−13 ± 70	**−16 ± 70**
Orthogonal	−56 ± 33	**−34 ± 33**
SMICA (T+E)		
Local	6.5 ± 5.0	**0.8 ± 5.0**
Equilateral	3 ± 43	**−4 ± 43**
Orthogonal	−36 ± 21	**−26 ± 21**

f_{NL} estimators comparison

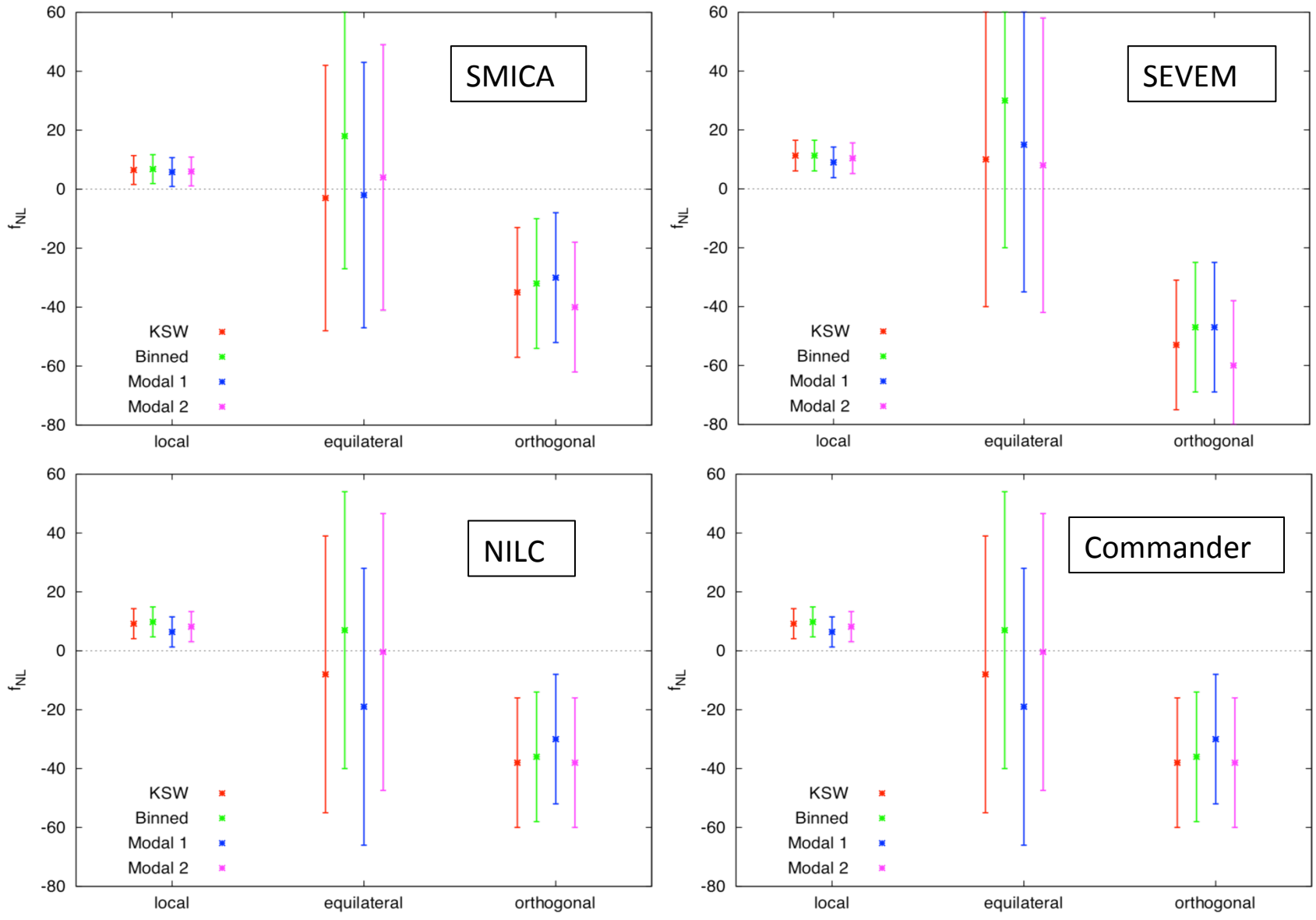

f_{NL} cleaned maps comparison (modal)

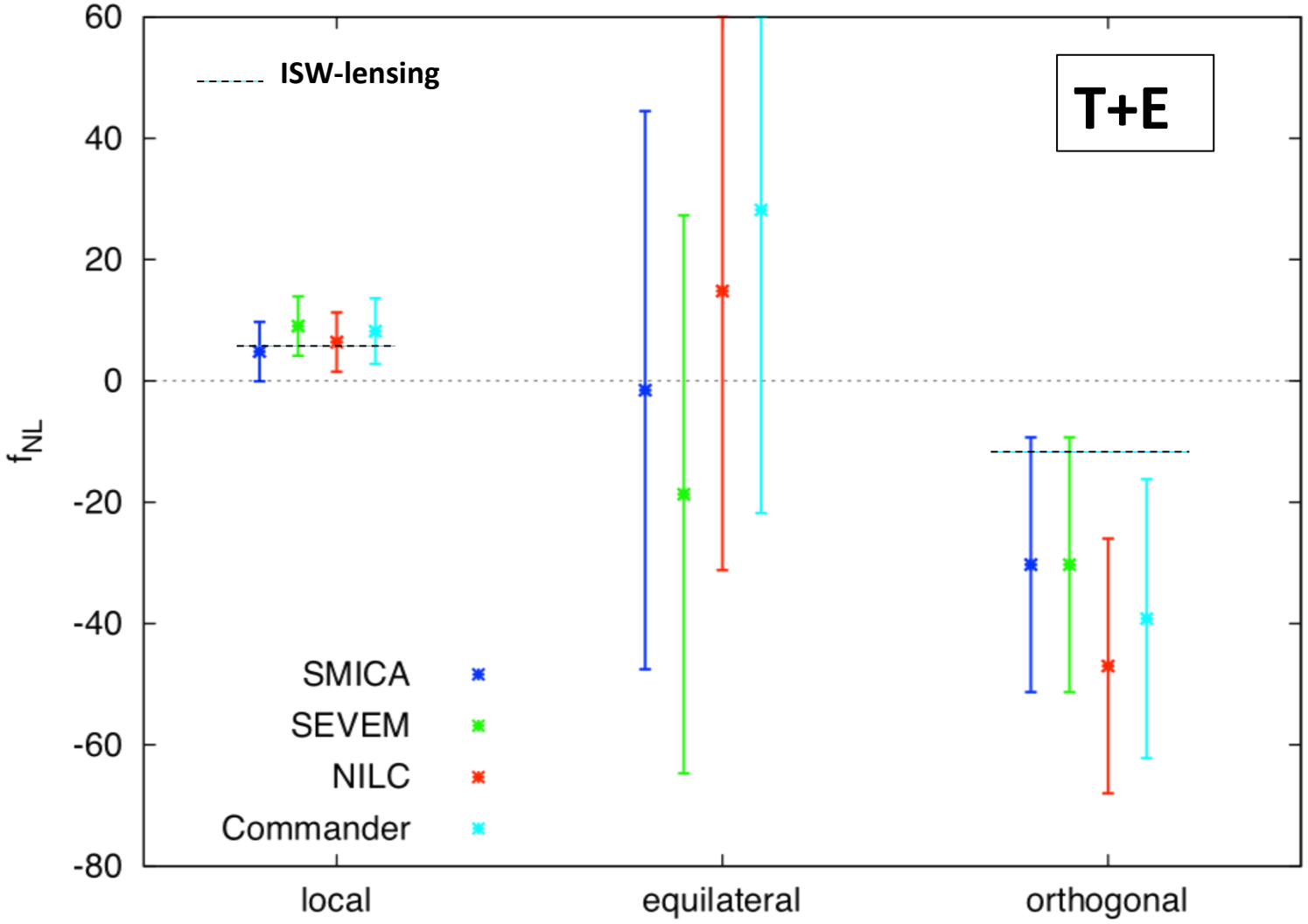

ISW-lensing bispectrum from *Planck* (2013)

The coupling between weak lensing and Integrated Sachs-Wolfe (ISW) effects is the leading contamination to local NG. We have detected the ISW lensing bispectrum with a significance of 2.6 σ

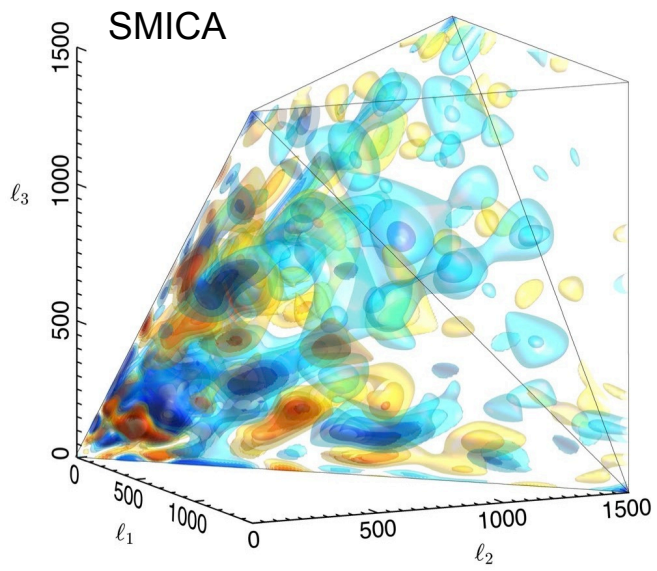

	SMICA	NILC	SEVEM	C-R
KSW	0.81 ± 0.31	0.85 ± 0.32	0.68 ± 0.32	0.75 ± 0.32
Binned	0.91 ± 0.37	1.03 ± 0.37	0.83 ± 0.39	0.80 ± 0.40
Modal	0.77 ± 0.37	0.93 ± 0.37	0.60 ± 0.37	0.68 ± 0.39

Results for the amplitude of the ISW-lensing bispectrum from the SMICA, NILC, SEVEM, and C-R foreground-cleaned maps, for the KSW, binned, and modal (polynomial) estimators; error bars are 68% CL.

Skew-C_l detection of ISW-lensing signal

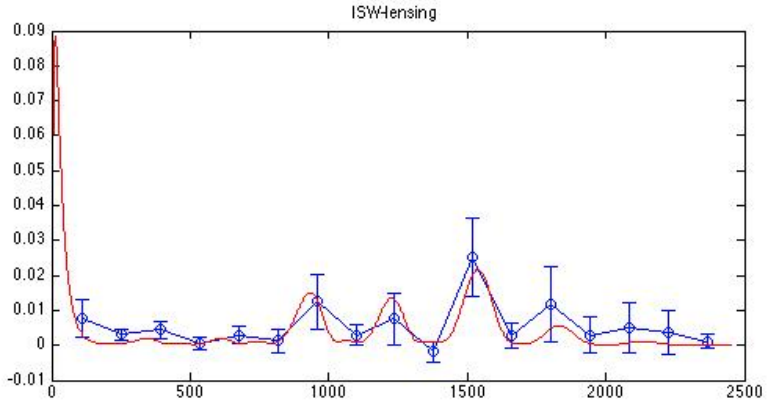

	SMICA	NILC	SEVEM	C-R
Local	7.1	7.0	7.1	6.0
Equilateral	0.4	0.5	0.4	1.4
Orthogonal	−22	−21	−21	−19

The bias in the three primordial fNL parameters due to the ISW-lensing signal for the 4 component-separation methods.

SMICA

Constraint on 4-point function from local NG (*Planck* 2013)

$\tau_{NL} < 2800$ @ 95% CL

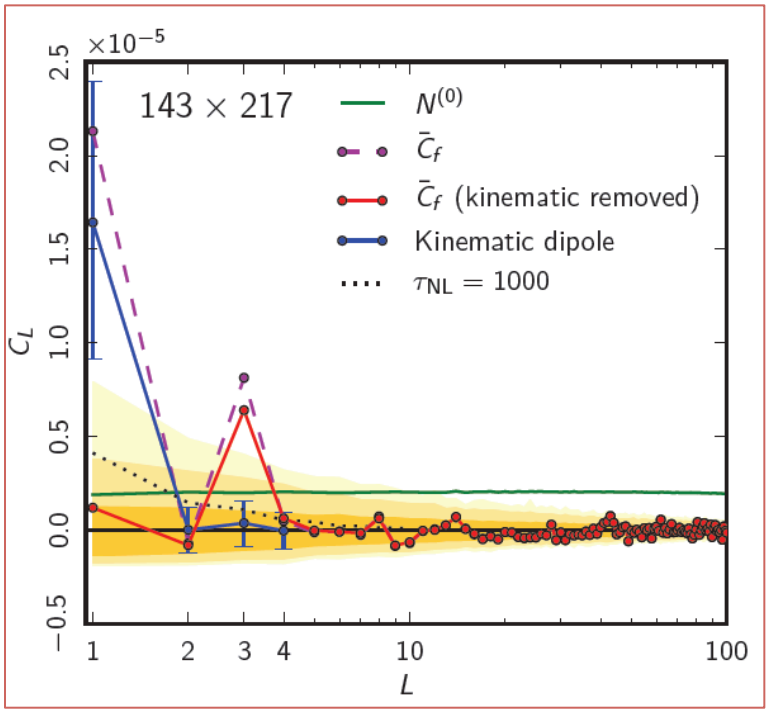

Power spectrum of the power modulation reconstructed from 143 X 217 GHz maps. Shading shows the 68%, 95% and 99% CL intervals from simulations with no modulation or kinematic signal. The dashed lines are when the mean field simulations include no kinematic eects, showing a clear detection of a modulation dipole. The blue points show the expected kinematic modulation dipole signal from simulations, along with 1σ error bars (only first four points shown for clarity). The solid line subtracts the dipolar kinematic signal in the mean fields from simulations including the expected signal, and represents out best estimate of the non-kinematic signal (note this is not just a subtraction of the power-spectra since the mean field takes out the fixed dipole anisotropy in real space before calculating the remaining modulation power). The dotted line shows the expected signal for $\tau_{NL} = 1000$.

Planck constraints on primordial trispectrum amplitudes

- In the 2015 release we obtained also constraints on 3 fundamental shapes of the trispectrum (transform of 4-pt function)

$$
\begin{aligned}
g_{\rm NL}^{\rm local} &= (-9.0 \pm 7.7) \times 10^4 \\
g_{\rm NL}^{\dot\sigma^4} &= (-0.2 \pm 1.7) \times 10^6 \\
g_{\rm NL}^{(\partial\sigma)^4} &= (-0.1 \pm 3.8) \times 10^5
\end{aligned}
$$

- We plan to extend this analysis in 2017 Planck analysis

Standard inflation is still alive
... and in very good shape!

Standard inflation i.e.

- single scalar field (*single clock*)
- canonical kinetic term
- slow-roll dynamics
- Bunch-Davies initial vacuum state
- Einstein gravity

predicts tiny (up to $O(10^{-2})$) primordial NG signal

→ no (presently) detectable primordial NG

Beyond “standard” shapes

In 2015 we constrained f_{NL} for a large number of primordial models beyond the standard local, equilateral, orthogonal shapes, including

- ✓ Equilateral family (DBI, EFT, ghost)
- ✓ Flattened shapes (non-Bunch Davies)
- ✓ Feature models (oscillatory bispectra, scale-dependent)
- ✓ Direction dependence
- ✓ Quasi-single-field
- ✓ Parity-odd models

- No evidence for NG found, constraints on parameters from the models above

- Extended survey of feature models with respect to 2013, 600 -> 2000 modes, including polarization.

Implications for inflation

- No evidence for primordial NG of the local, equilateral, orthogonal type. consistent with the simplest scenario: standard single-field slow roll.
- Other possibilities are however not ruled out. Constraints on f_{NL} are converted into constraints on relevant model parameters, for example:

  - Curvaton decay fraction $r_D > 19\%$ (from local $f_{NL,}$ T+E)

  - Speed of sound in Effective Field Theory $c_S > 0.024$ (from equil. + ortho. f_{NL})

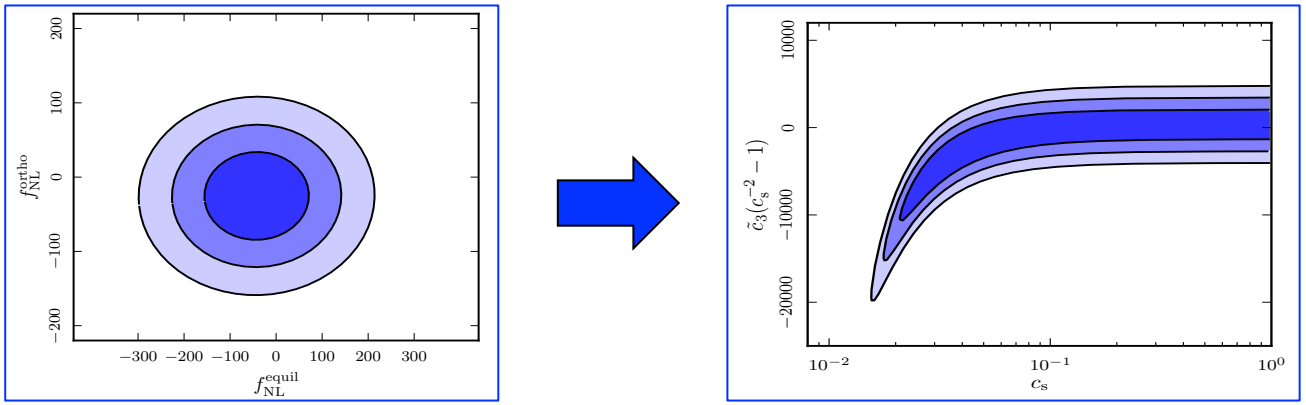

  - DBI inflation: $c_S > 0.087$ (T+E)

Summary of *Planck* 2015 results on PNG

- Constraints on local, equilateral, orthogonal bispectra improved by up to 15% w.r.t. 2013
- First PNG analysis using polarization data
- Constraints on T+E (2015) confirm T results with significantly reduced error bars
- 2013 hints of NG in oscillatory feature models remain in T, but decrease significantly when polarization is included; look-elsewhere effect fully accounted for; new estimator for high-frequency oscillations covering 10 times more parameter space
- New constraints on:
  - isocurvature NG: polarizartion data crucial in this respect
  - tensor NG analyzed: parity-odd T limit consistent with WMAP (and with null result)
  - trispectrum due to cubic NG (g_{NL} for a variety of shapes)
- 2015 analysis contains largely extended analysis of NG templates
- → 2017 analysis ("*Planck* legacy" paper) will further improve on standard shapes (owing to refined treatment of E-mode polarization maps), add some extra shapes (scale-dependent f_{NL}, conformal symmetry, …). Search for features in both PS and bispectrum.

PNG with CMB spectral distortions

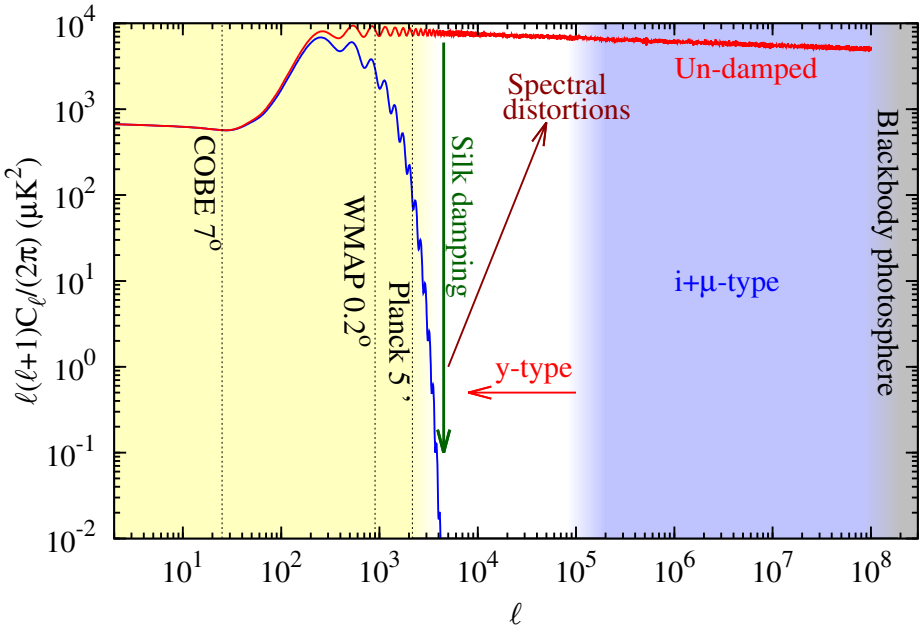

CMB spectral distortions from acoustic wave dissipation probe a large range of scales, much more than CMB/LSS

Many additional modes!

Kathri & Sunyaev 2013, arXiv: 1303.7212

If μ-*anisotropies* are measured ($\delta\mu \sim \Phi^2$):

- ✓ Tμ correlation: primordial local f_{NL} (Pajer & Zaldarriaga 2013)
  or other squeezed shapes, e.g. excited initial states (Ganc & Komatsu 2013)
- ✓ μμ correlation: primordial local trispectrum, τ_{NL} (Bartolo, Liguori, Shiraishi 2016)
- ✓ TTμ bispectrum: primordial local trispectrum, g_{NL} (Bartolo, Liguori, Shiraishi 2016)

Credits: M. Liguori

PNG with CMB spectral distortions

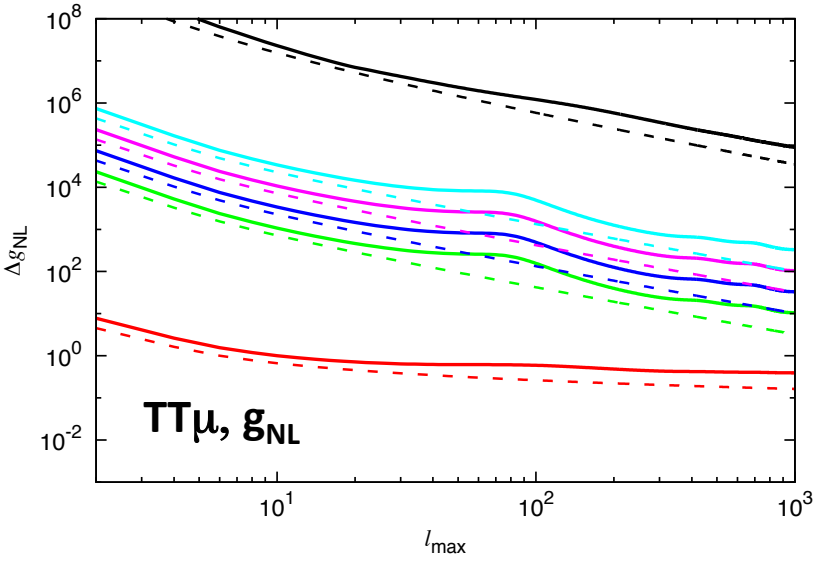

For Gaussian initial conditions, dissipated power in small patches is isotropically distributed

If local NG is present, large scale modulation of the small-scale power arise => Tm correlations (Pajer, Zaldarriaga 2013, Emami et al. 2015)

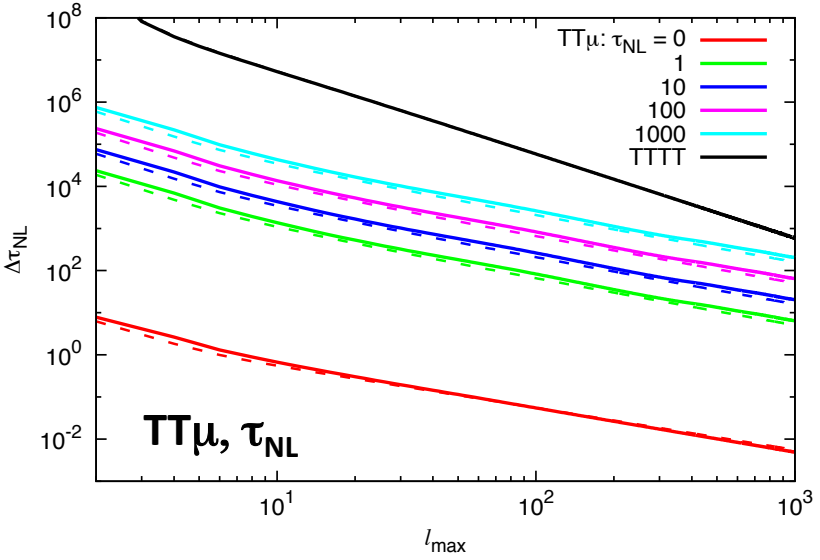

$$\Phi = \Phi_G + \Phi_{NG} = \Phi_G + f_{NL}\Phi_G^2,$$

$$\Phi_G = \Phi_S + \Phi_L \Rightarrow \Phi_{NG} = \Phi_S^2 + \Phi_L^2 + 2 f_{NL}\Phi_S\Phi_L$$

$$\Phi \propto \Phi_S\left(1 + 2 f \Phi_L\right) \Rightarrow \frac{\delta\left\langle \Phi^2 \right\rangle}{\Phi^2} = \frac{\delta\mu}{\mu} \sim 4 f_{NL}\Phi_L$$

$$\Rightarrow \left\langle \frac{\delta T}{T}\bigg|_L \frac{\delta\mu}{\mu} \right\rangle \propto f_{NL} C_\ell$$

Bartolo, Liguori & Shiraishi 2016

Chern-Simons gravitational term

Bartolo & Orlando 2017

Lagrangian:

$$\mathcal{L} = \sqrt{g}\left[\frac{1}{2}M_{Pl}^2 R - \frac{1}{2}g^{\mu\nu}\partial_\mu\phi\partial^\mu\phi - V(\phi)\right] + f(\phi)\epsilon^{\mu\nu\rho\sigma}C_{\mu\nu}{}^{\kappa\lambda}C_{\rho\sigma\kappa\lambda}$$

Weyl tensor

The Chern-Simons term arises from an effective field theory expansion of the fundamental theory

Peculiarities of the Chern-Simons gravitational term

Parity breaking

Vanishing in the background $\left(C^{(0)}_{\mu\nu\rho\sigma} = 0\right)$

Invariant under a Weyl transformation of the metric $g' = e^{-2w(x,t)}g$

Surface term without the coupling function f(φ)

Effects on PGW

$$S|_{\gamma\gamma} = \sum_{s=L,R} \int d\tau \, \frac{d^3k}{(2\pi)^3} \, A_{T,s}^2 \left[\, |\gamma_s'(\tau,k)|^2 - k^2 |\gamma_s(\tau,k)|^2 \, \right]$$

$$A_{T,s}^2 = \frac{M_{pl}^2}{2} a^2 \left(1 - 8\lambda_s \frac{k}{a} \frac{\dot{f}(\phi)}{M_{pl}^2} \right) = a^2 \left(1 - \lambda_s \frac{k_{phys}}{M_{CS}} \right)$$

$$M_{CS} = \frac{M_{pl}^2}{8\dot{f}(\phi)}$$

$\lambda_R = +1$, $\lambda_L = -1$

Right-handed PGW become GHOST fields when $k_{phys} > M_{CS}$

SOLUTION: put an UV energy cut-off in the theory

Parity breaking signatures in tensor power spectrum are suppressed

bispectrum: two gravitons-one scalar correlator has interesting features

i. Parity breaking signatures are not suppressed
ii. squeezed shape

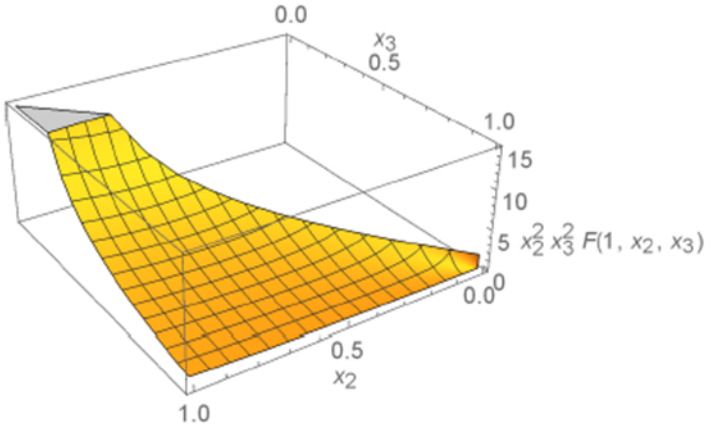

Enhancing SST

TSS bispectrum model

Shiraishi, Liguori, Fergusson 2017

- TSS bispectrum (λ = elicity, g_{tss} = NG amplitude)

$$\left\langle \gamma^{(\lambda_1)}_{\mathbf{k}_1} \zeta_{\mathbf{k}_2} \zeta_{\mathbf{k}_3} \right\rangle = (2\pi)^3 \delta^{(3)} \left(\sum_{n=1}^{3} \mathbf{k}_n \right) e^{(-\lambda_1)}_{ij}(\hat{k}_1) \hat{k}_{2i} \hat{k}_{3j} \frac{16\pi^4 g_{tss} A_S^2}{k_1^2 k_2^2 k_3^2} \frac{I_{k_1 k_2 k_3}}{k_1}$$

- Shape

$$I_{k_1 k_2 k_3} \equiv -k_t + \frac{k_1 k_2 + k_2 k_3 + k_3 k_1}{k_t} + \frac{k_1 k_2 k_3}{k_t^2}$$

- Realized also in standard single-field, but gtss is small (~ ε). Can be enhanced with non-zero mass of gravitons

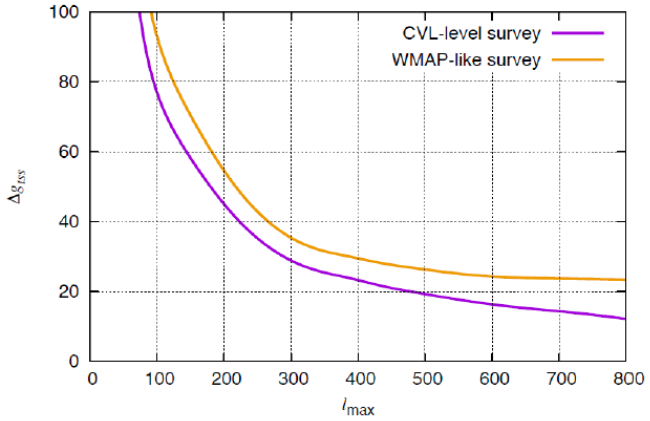

Not much improvement allowed. Need B-modes and TTB (TBB

Shape

- CMB shape takes a complex, non-separable from. Can be expanded e.g. via modal decompositions. Local-type NG

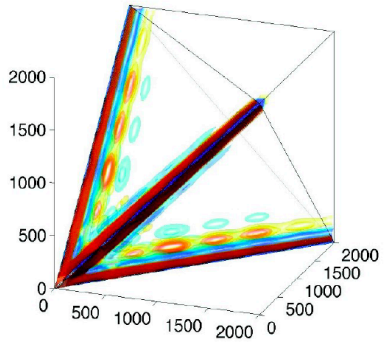

also Bartolo et al. 2015

- WMAP 9-yrs bounds (as a function of lmax)

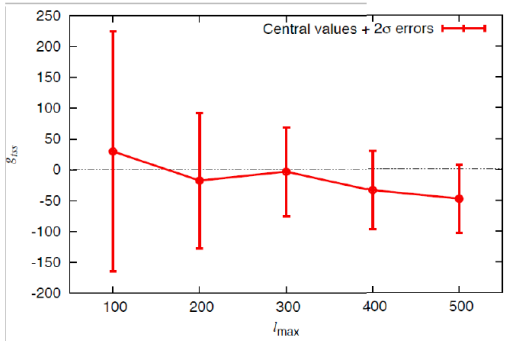

$-76 < g_{tss} < -20$ (68% C.L.) (Shiraishi, Liguori, Fergusson 2017)

CORE: CMB bispectrum forecasts

	LiteCORE 80	LiteCORE 120	**CORE M5**	COrE+	Planck 2015	LiteBIRD	ideal 3000
T local	4.5	3.7	**3.6**	3.4	(5.7)	9.4	2.7
T equilat	65	59	**58**	56	(70)	92	46
T orthog	31	27	**26**	25	(33)	58	20
T lens-isw	0.15	0.11	**0.10**	0.09	(0.28)	0.44	0.07
E local	5.4	4.5	**4.2**	3.9	(32)	11	2.4
E equilat	51	46	**45**	43	(141)	76	31
E orthog	24	21	**20**	19	(72)	42	13
E lens-isw	0.37	0.29	**0.27**	0.24		1.1	0.14
T+E local	2.7	2.2	**2.1**	1.9	(5.0)	5.6	1.4
T+E equilat	25	22	**21**	20	(43)	40	15
T+E orthog	12	10.0	**9.6**	9.1	(21)	23	6.7
T+E lens-isw	0.062	0.048	**0.045**	0.041		0.18	0.027

from: Finelli et al. 2016

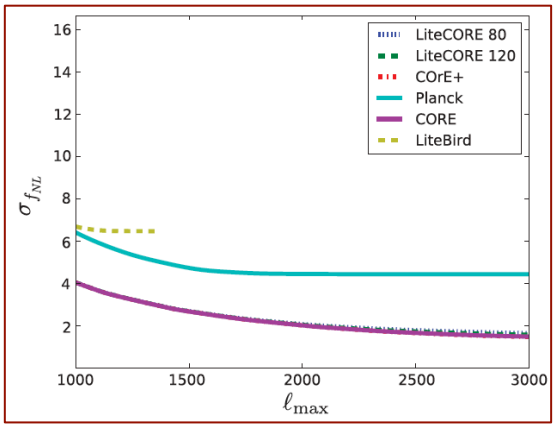

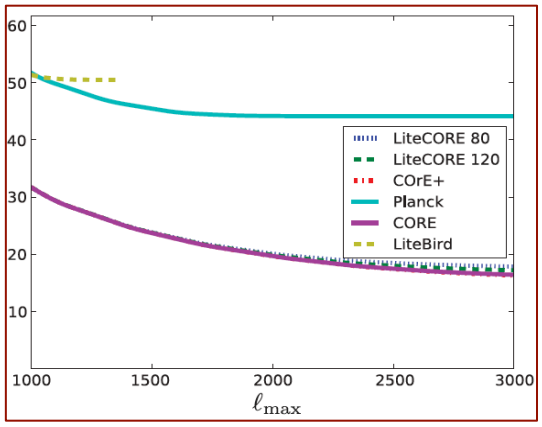

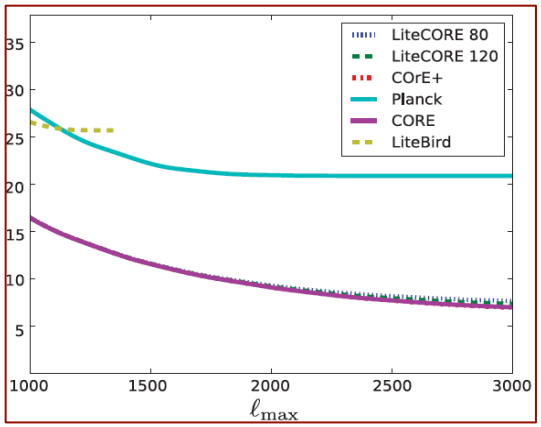

Primordial Non-Gaussianity (PNG) & the Large-Scale Structure (LSS) of the Universe

(= primordial NG + NG from gravitational instability)

PNG and LSS

PNG in LSS (to make contact with the CMB definition) can be defined through a potential Φ defined starting from the DM density fluctuation δ through Poisson's equation (use comoving gauge for density fluctuation, Bardeen 1980)

$$\delta = -\left(\frac{3}{2}\Omega_m H^2\right)^{-1} \nabla^2 \Phi$$

Assuming the same model

$$\Phi = \phi_L + f_{NL}(\phi_L^2 - \langle\phi_L^2\rangle) + g_{NL}(\phi_L^3 - \langle\phi_L^2\rangle\phi_L) + \ldots$$

Φ on sub-horizon scales reduces to minus the large-scale gravitational potential, ϕ_L is the linear Gaussian contribution and f_{NL} and g_{NL} are dimensionless non-linearity parameters (or more generally non-linearity functions).

CMB and LSS conventions may differ by a factor 1.3 for f_{NL}, $(1.3)^2$ for g_{NL}

Searching for PNG with rare events

- Besides using standard statistical estimators, like (mass) bispectrum, trispectrum, three and four-point function, skewness, etc. …, one can look at the tails of the distribution, i.e. at rare events.

- Rare events have the advantage that they often maximize deviations from what is predicted by a Gaussian distribution, but have the obvious disadvantage of being rare! But remember that, according to Press-Schechter-like schemes, all collapsed DM halos correspond to (rare) high peaks of the underlying density field (note: density, not gravitational potential maxima).

- Matarrese, Verde & Jimenez (2000) and Verde, Jimenez, Kamionkowski & Matarrese showed that clusters at high redshift (z>1) can probe NG down to $f_{NL} \sim 10^2$. Alternative approach by LoVerde et al. (2007). Determination of mass function using stochastic approach (first-crossing of a diffusive barrier) Maggiore & Riotto 2009. Ellipsoidal collapse used by Lam & Sheth 2009. Saddle-point + diffusive barrier (Paranjape et al. 2010). Log-Edgeworth expantion: LoVerde & Smith 2011. Excursion sets studied with correlated steps: Paranjape, Lam & Sheth 2011; Paranjape & Sheth 2011, ... and many, many more. Excellent agreement of analytical formulae with N-body simulations found by Grossi et al. 2009; Desjacques et al. 2009; Pillepich et al. 2010; … and many others afterwards.

- Halo (galaxy) clustering and halo (galaxy) higher-order correlation functions represent further and more powerful implementations of this general idea.

NG vs halo mass function

- The halo mass function (à-la-Press-Schechter) can be a useful tool to probe PNG as it essentially depends exponentially on the PNG parameters (Matarrese, Verde & Jimenez 2000), by modulating the critical overdensity for collapse. Its calculation can be done along the lines of the original PS approach, using a steepest-descent approximation to deal with (small) PNG.

NG vs. halo mass function

- Relevant effects:
  - non-Markovianity, already there in the Gaussian case, unavoidable in NG case
  - non-spherical collapse
  - connecting random walks w. DM halos
- Dealing with rare events i.e. tails of NG distribution
- Validation with N-body simulations crucial (although very rare events/tails not probed by finite number of realizations → analytical treatments welcome!)
- Understanding/definition of connection between analytical/numerical quantities and real observables → to what level is this affecting NG (e.g. f_{NL}) measurements?
- A more fundamental question: should we necessarily go on with (extended) Press-Schechter-like approaches? Are alternative approaches viable: e.g. Smoluchowski equation for non-Poissonian random process (earliest attempt by Silk & White 1978)

Different approaches to the NG halo mass function

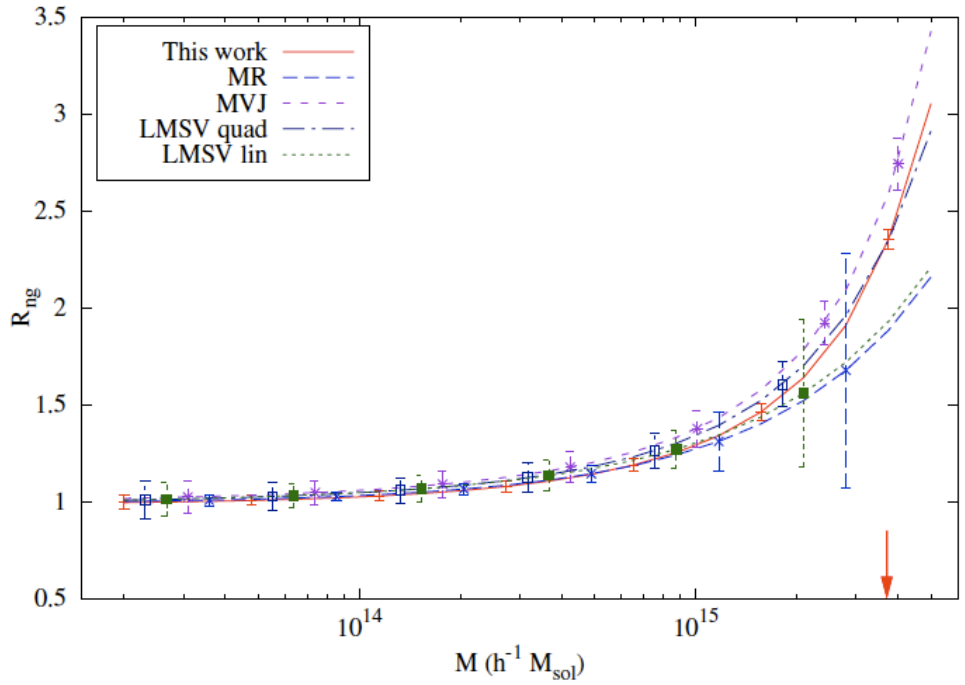

Figure 6: Same as Fig. 5, but including filter effects. These affect only the error bars for MVJ and LMSV, and they affect both the curve and the error bars for MR and our result. For MR and our result, the Gaussian mass function used to construct the ratio $R_{\rm ng}$, is taken as the non-Gaussian result at $f_{\rm NL} = 0$, and hence includes filter effects.

Paranjape et al. 2010

Bias: halos (➔galaxies) do not trace the underlying (dark) matter distribution

- Following the original proposal by Kaiser (1984), introduced for galaxy clusters and later for galaxies, we are used to parametrize our ignorance about the way in which DM halos clusters in space w.r.t. the underlying DM, via some "bias" parameters, e.g. (Eulerian bias)

- $\delta_{halo}(x) = b_1 \delta_{matter}(x) + b_2 \delta^2_{matter}(x) + \ldots$

- or via some non-linear and non-local expression (e.g. as a function of the Lagrangian position of the proto-halo center of mass.
- The resulting non-linear and non-local affects the statistical distribution of the halos introducing further NG effects.
- The various bias parameters can be generally dealt with either as purely phenomenological ones (i..e. to be fitted to observations) or predicted by a theory (e.g. Press-Schechter + Lagrangian PT).

Dark matter halo clustering as a powerful constraint on PNG

$$\delta_{halo} = b\, \delta_{matter}$$

Dalal et al. (2007) have shown that halo bias is sensitive to primordial non-Gaussianity through a scale-dependent correction term (in Fourier space)

$$\Delta b(k)/b \;\alpha\; 2\, f_{NL} \delta_c / k^2$$

This opens interesting prospects for constraining or measuring NG in LSS but demands for an accurate evaluation of the effects of (general) NG on halo biasing.

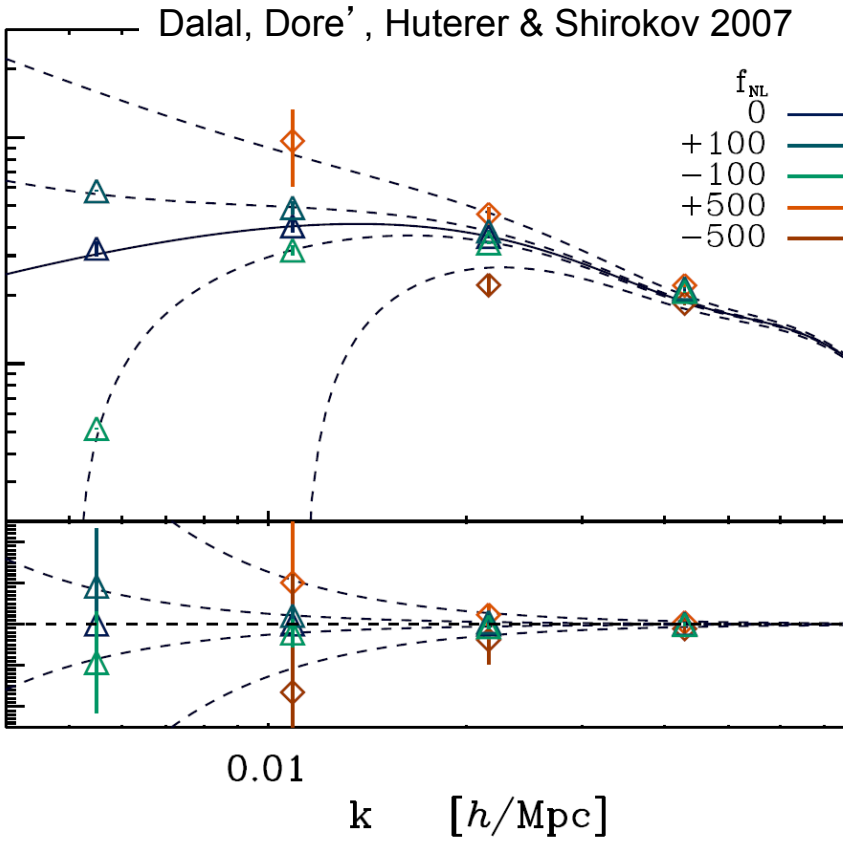

Clustering of peaks (DM halos) of NG density field

Start from results obtained in the 80's by Grinstein & Wise 1986, ApJ, 310, 19; Matarrese, Lucchin & Bonometto 1986, ApJ, 310, L21 giving the general expression for the peak 2-point function as a function of N-point connected correlation functions of the background linear (i.e. Lagrangian) mass-density field

$$\xi_{h,M}\left(|\mathbf{x}_1 - \mathbf{x}_2|\right) = -1 +$$

$$\exp\left\{\sum_{N=2}^{\infty}\sum_{j=1}^{N-1}\frac{\nu^N\sigma_R^{-N}}{j!(N-1)!}\xi^{(N)}\begin{bmatrix}\mathbf{x}_1,\ldots,\mathbf{x}_1, & \mathbf{x}_2,\ldots\ldots,\mathbf{x}_2\\ j\ times & (N-j)\ times\end{bmatrix}\right\}$$

(requires use of path-integral, cluster expansion, multinomial theorem and asymptotic expansion). The analysis of NG models was motivated by a paper by Vittorio, Juszkiewicz and Davis (1986) on bulk flows.

THE ASTROPHYSICAL JOURNAL, 310:L21–L26, 1986 November 1

A PATH-INTEGRAL APPROACH TO LARGE-SCALE MATTER DISTRIBUTION ORIGINATED BY NON-GAUSSIAN FLUCTUATIONS

SABINO MATARRESE
International School for Advanced Studies, Trieste, Italy
FRANCESCO LUCCHIN
Dipartimento di Fisica G. Galilei, Padova, Italy
AND
SILVIO A. BONOMETTO
International School for Advanced Studies, Trieste, Italy; Dipartimento di Fisica G. Galilei, Padova, Italy; and INFN, Sezione di Padova
Received 1986 July 7; accepted 1986 August 1

ABSTRACT

The possibility that, in the framework of a biased theory of galaxy clustering, the underlying matter distribution be non-Gaussian itself, because of the very mechanisms generating its present status, is explored. We show that a number of contradictory results, seemingly present in large-scale data, in principle can recover full coherence, once the requirement that the underlying matter distribution be Gaussian is dropped. For example, in the present framework the requirement that the two-point correlation functions vanish at the same scale (for different kinds of objects) is overcome. A general formula, showing the effects of a non-Gaussian background on the expression of three-point correlations in terms of two-point correlations, is given.

Subject heading: galaxies: clustering

HE ASTROPHYSICAL JOURNAL, 310:19–22, 1986 November 1

NON-GAUSSIAN FLUCTUATIONS AND THE CORRELATIONS OF GALAXIES OR RICH CLUSTERS OF GALAXIES[1]

BENJAMIN GRINSTEIN[2] AND MARK B. WISE[3]
California Institute of Technology
Received 1986 March 6; accepted 1986 April 18

ABSTRACT

Natural primordial mass density fluctuations are those for which the probability distribution, for mass density fluctuations averaged over the horizon volume, is independent of time. This criterion determines that the two-point correlation of mass density fluctuations has a Zeldovich power spectrum (i.e., a power spectrum proportional to k at small wavenumbers) but allows for many types of reduced (connected) higher correlations. Assuming galaxies or rich clusters of galaxies arise wherever suitably averaged natural mass density fluctuations are unusually large, we show that the two-point correlation of galaxies or rich clusters of galaxies can have significantly more power at small wavenumbers (e.g., a power spectrum proportional to $1/k$ at small wavenumbers) than the Zeldovich spectrum. This behavior is caused by the non-Gaussian part of the probability distribution for the primordial mass density fluctuations.

Subject headings: cosmology — galaxies: clustering

Halo bias in NG models

- Matarrese & Verde 2008 applied this relation to the case of NG of the gravitational potential, obtaining the power-spectrum of dark matter halos modeled as high "peaks" (up-crossing regions) of height $\nu=\delta_c/\sigma_R$ of the underlying mass density field (Kaiser's model). Here $\delta_c(z)$ is the critical overdensity for collapse (at redshift a) and σ_R is the *rms* mass fluctuation on scale R ($M \sim R^3$).

- Account for motion of peaks (going from Lagrangian to Eulerian space), which implies (Catelan et al. 1998)

$$1+\delta_h(\mathbf{x}_{Eulerian}) = (1+\delta_h(\mathbf{x}_{Lagrangian}))(1+\delta_R(\mathbf{x}_{Eulerian}))$$

and (to linear order) $b=1+b_L$ (Mo & White 1996) to get the scale-dependent halo bias in the presence of NG initial conditions. *Corrections may arise from second-order bias and GR terms.*

- Alternative approaches (e.g. based on 1-loop calculations) by Taruya et al. 2008; Matsubara 2009; Jeong & Komatsu 2009. Giannantonio & Porciani 2010 improve fit to N-body simulations by assuming dependence on gravitational potential) → extension to bispectrum by Baldauf et al. 2011. Leistedt et al. (2014) include g_{NL} and f_{NL} in analysis os QSO clustering.

Halo bias in NG models

- Extension to general (scale and configuration dependent) NG is Straightforward (Matarrese & Verde 2008)

- In full generality write the f bispectrum as $B_f(k_1,k_2,k_3)$. The relative NG correction to the halo bias is

$$\frac{\Delta b_h}{b_h} = \frac{\Delta_c(z)}{D(z)} \frac{1}{8\pi^2\sigma_R^2} \int dk_1 k_1^2 \mathcal{M}_R(k_1) \times$$
$$\int_{-1}^{1} d\mu \mathcal{M}_R\left(\sqrt{\alpha}\right) \frac{B_\phi(k_1, \sqrt{\alpha}, k)}{P_\phi(k)} \times \frac{1}{M_R(k)}$$

$$\alpha = k_1^2 + k^2 + 2k_1 k\mu$$

- It also applies to non-local (e.g. "equilateral") PNG (DBI, ghost inflation, etc..) and universal PNG term!! (→ see also Schmidt & Kamionkowski 2010).

Halo bias in NG models

Matarrese & Verde 2008

$$b_{\rm h}^{f_{\rm NL}} = 1 + \frac{\Delta_c(z)}{\sigma_R^2 D^2(z)} \left[1 + 2 f_{\rm NL} \frac{\Delta_c(z)}{D(z)} \frac{\mathcal{F}_R(k)}{\mathcal{M}_R(k)} \right]$$

form factor:

$$\mathcal{F}_R(k) = \frac{1}{8\pi^2 \sigma_R^2} \int dk_1 k_1^2 \mathcal{M}_R(k_1) P_\phi(k_1) \times \int_{-1}^{1} d\mu \mathcal{M}_R\left(\sqrt{\alpha}\right) \left[\frac{P_\phi\left(\sqrt{\alpha}\right)}{P_\phi(k)} + 2 \right]$$

$$\alpha = k_1^2 + k^2 + 2 k_1 k \mu$$

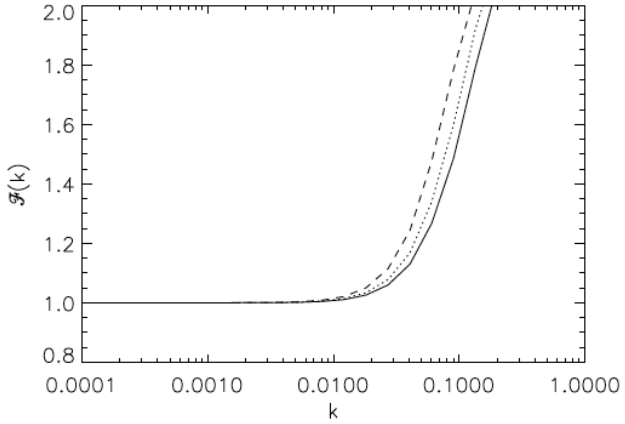

FIG. 1.— The function $\mathcal{F}_R(k)$ for three different masses: 1×10^{14} $M_\odot$ (solid), 2×10^{14} $M_\odot$ (dotted), 1×10^{15} $M_\odot$ (dashed).

factor connecting the smoothed linear overdensity with the primordial potential:

power-spectrum of a Gaussian gravitational potential

$$\mathcal{M}_R(k) = \frac{2}{3} \frac{T(k) k^2}{H_0^2 \Omega_{m,0}} W_R(k)$$

transfer function:

window function defining the radius R of a proto-halo of mass M(R):

PNG with LSS: 2-point function

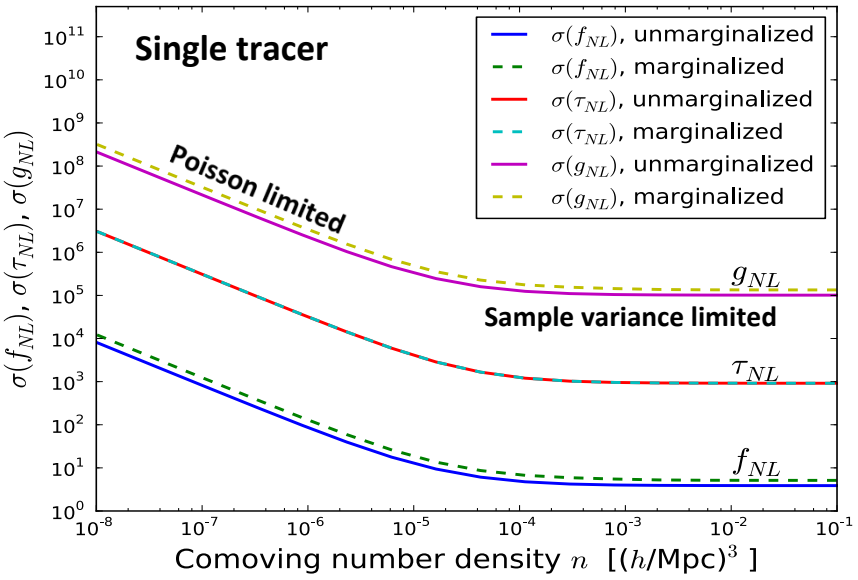

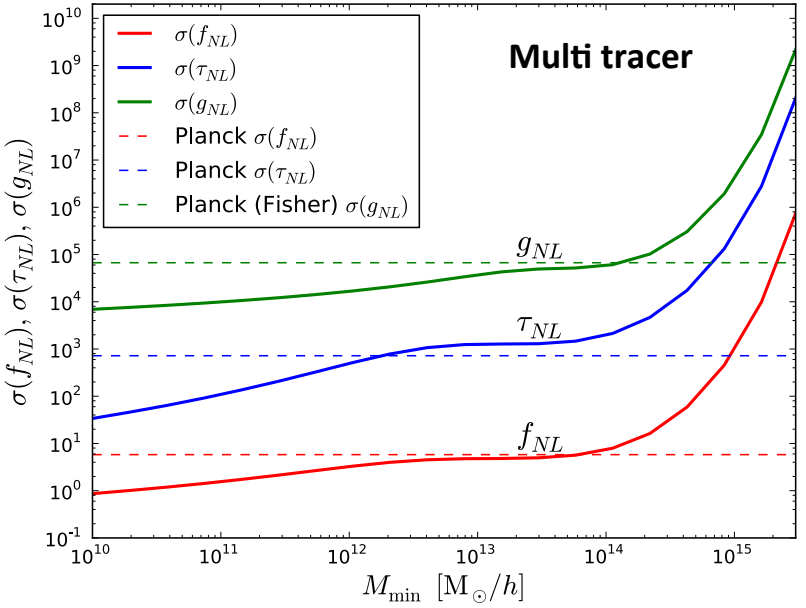

Ferraro & Smith 2014

$$\Delta b(k) = 2(b-1) f_{\mathrm{NL}} \delta_c \frac{3\Omega_m}{2a\, g(a) r_H^2 k^2}$$

- Single tracer, V = 25 Gpc^3 h^{-3}, statistical power ~ Planck
- Multi-tracer techniques have the power to reach σ_{fNL} ~ 1 (local)
- Significant degeneracies between f_{NL}, g_{NL}, τ_{NL}

Credits: M. Liguori

CIB power spectrum

- CIB power spectrum is integrated over a large volume. Ideal for scale dependent bias **(Tucci et al. 2016)**
- Seriously contaminated by dust, but future full-sky satellite B-mode experiments with many (high-)frequency channels allow very accurate component separation.

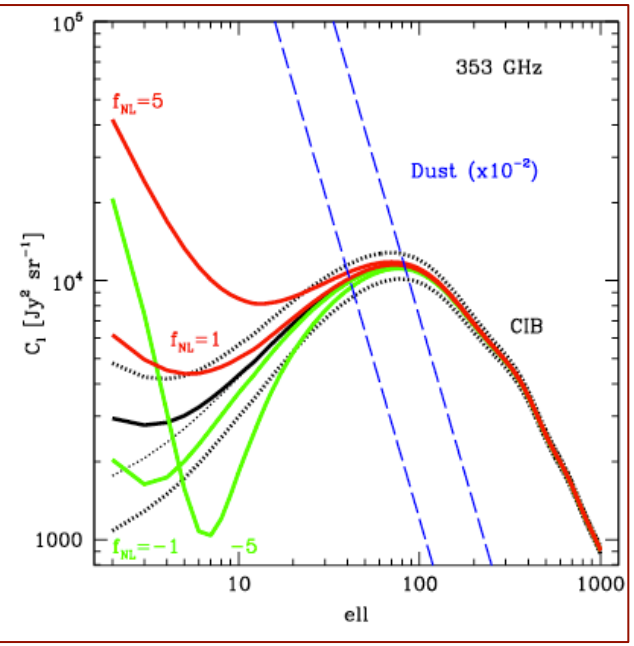

(Tucci et al. 2016)

									$\sigma(f_{NL})$
COrE+									
ν [GHz]	220	255	295	340	390	450	520	600	
fwhm [arcmin]	3.82	3.29	2.85	2.47	2.15	1.87	1.62	1.40	
w^{-1} [Jy^2 sr^{-1}]	0.654	1.43	5.20	8.31	13.50	22.98	39.88	69.26	
Σ^2_{CIB} [Jy^2 sr^{-1}]	–	8.04	–	47.3	–	212.	382.	–	**1.6**
COrE+ with *Planck*									
Σ^2_{CIB} [Jy^2 sr^{-1}]	–	1.97	–	10.8	–	45.6	90.2	163.6	**0.6**
CORE									$\sigma(f_{NL})$
ν [GHz]	220	255	295	340	390	450	520	600	
fwhm [arcmin]	5.23	4.57	3.99	3.49	3.06	2.65	2.29	1.98	
w^{-1} [Jy^2 sr^{-1}]	0.29	0.57	0.77	1.08	2.16	3.55	6.2	11.0	
Σ^2_{CIB} [Jy^2 sr^{-1}]	–	1.8	–	8.8	–	42.9	80.1	–	**0.7**
CORE with *Planck*									
Σ^2_{CIB} [Jy^2 sr^{-1}]	–	1.03	–	5.2	–	23.3	43.9	68.9	**0.34**

(Finelli et al. 2016)

Credits: M. Liguori

PNG with LSS: the galaxy bispectrum

Let's follow Tellarini et al. (2016)

The linearly evolving density field $\delta_{\rm lin}$ is related to the primordial gravitational potential through

$$\delta_{\rm lin}(\mathbf{k}, z) = \alpha(k, z)\Phi_{\rm in}(\mathbf{k})\,,$$

where the function $\alpha(k, z)$ is defined as

$$\alpha(k, z) \equiv \frac{2k^2c^2T(k)D(z)}{3\Omega_m H_0^2}\,.$$

$T(k)$ is the transfer function, which goes to one as $k \to 0$. Note that the linearly evolving density (eq. (2.3)) includes non-Gaussian terms in the presence of PNG. Thus it is useful to define the Gaussian part of the linearly evolving density field as

$$\delta_{\rm G}(\mathbf{k}, z) = \alpha(k, z)\varphi_{\rm G}(\mathbf{k})\,.$$

Second-order (Eulerian) PT yields:

$$\delta^{(2)}(\mathbf{k}, z) = \int \frac{d\mathbf{k}_1}{(2\pi)^3} \int \frac{d\mathbf{k}_2}{(2\pi)^3}\, \delta^D(\mathbf{k} - \mathbf{k}_1 - \mathbf{k}_2) \left[\mathcal{F}_2(\mathbf{k}_1, \mathbf{k}_2) + f_{\rm NL}\frac{\alpha(k)}{\alpha(k_1)\alpha(k_2)}\right] \delta_{\rm G}(\mathbf{k}_1, z)\delta_{\rm G}(\mathbf{k}_2, z)$$

with the 2-nd order gravity-kernel $\quad \mathcal{F}_2(\mathbf{k}_1, \mathbf{k}_2) = \frac{5}{7} + \frac{1}{2}\frac{\mathbf{k}_1 \cdot \mathbf{k}_2}{k_1 k_2}\left(\frac{k_1}{k_2} + \frac{k_2}{k_1}\right) + \frac{2}{7}\frac{(\mathbf{k}_1 \cdot \mathbf{k}_2)^2}{k_1^2 k_2^2}$

PNG with LSS: the galaxy bispectrum

The quantity δ(x) is expressed in Eulerian frame, with the initial spatial coordinate $\mathbf{q}$ in the Lagrangian frame being related to the evolved Eulerian coordinate $\mathbf{x}$ through the formula

$$\mathbf{x}(\mathbf{q},\tau) = \mathbf{q} + \mathbf{\Psi}(\mathbf{q},\tau)\,,$$

where $\mathbf{\Psi}$ is the displacement field. Such relation is useful for obtaining an alternative way to write the second-order solution of eq. (2.6), which will be needed in section 2.4. It is given by [61, 62]:

$$\delta^{(2)}(\mathbf{x},\tau) = \frac{17}{21}(\delta_{\rm lin}(\mathbf{x},z))^2 + \frac{2}{7}s^2(\mathbf{x},z) - \mathbf{\Psi}(\mathbf{x},z)\cdot\nabla\delta(\mathbf{x},z)\,,$$

where $s^2 = s_{ij}s^{ij}$ and s_{ij} is the trace-free *tidal tensor*, defined as

$$s_{ij} \equiv \left(\nabla_i\nabla_j - \frac{1}{3}\delta^K_{ij}\nabla^2\right)\nabla^{-2}\delta\,,$$

and δ^K_{ij} is the Kronecker delta. From now on, in order to simplify our expressions, we will not explicitly write the redshift dependence in the density and velocity fields.

PNG with LSS: the galaxy bispectrum

One can introduce a long-short splitting of the gravitational potential and DM density field, such that, for local NG one easily finds (for local NG)

$$\delta_{\mathrm{lin},l}(\mathbf{k}) = \delta_{\mathrm{G},l} + f_{\mathrm{NL}}\alpha\left(\varphi^2_{\mathrm{G},l} - \langle\varphi^2_{\mathrm{G},l}\rangle\right)$$

with

$$\varphi_{\mathrm{G}}(\mathbf{q}) = \varphi_{\mathrm{G},l}(\mathbf{q}) + \varphi_{\mathrm{G},s}(\mathbf{q})$$

In Lagrangian space one can then introduce the expansion

$$\delta^{\mathrm{L}}_g(\mathbf{q}) = \frac{n_g(\mathbf{q}) - \langle n_g\rangle}{\langle n_h\rangle} = b^{\mathrm{L}}_{10}\delta_{\mathrm{lin}} + b^{\mathrm{L}}_{01}\varphi_{\mathrm{G}} + b^{\mathrm{L}}_{20}(\delta_{\mathrm{lin}})^2 + b^{\mathrm{L}}_{11}\delta_{\mathrm{lin}}\varphi_{\mathrm{G}} + b^{\mathrm{L}}_{02}\varphi^2_{\mathrm{G}} + \dots,$$

where the subscript l has been dropped and the 5 b_{ij} represent our (generally unknown) bias parameters

PNG with LSS: the galaxy bispectrum

One can then move to the final Eulerian position of the galaxy by using the conservation law (Catelan et al. 1998)

$$1+\delta_g^{\rm E}(\mathbf{x},z)=\left[1+\delta(\mathbf{x},z)\right]\left[1+\delta_g^{\rm L}(\mathbf{q},z)\right]$$

to find

$$\delta_g^{\rm E}(\mathbf{k})=b_{10}^{\rm E}\delta+b_{01}^{\rm E}\varphi_{\rm G}+b_{20}^{\rm E}\delta*\delta+b_{11}^{\rm E}\delta*\varphi_{\rm G}+b_{02}^{\rm E}\varphi_{\rm G}*\varphi_{\rm G}-\frac{2}{7}b_{10}^{\rm L}s^2-b_{01}n^2$$

where s^2 and n^2 are suitable expansion terms and the Eulerian bias parameters read:

$$\begin{aligned}
b_{10}^{\rm E}&=1+b_{10}^{\rm L}\,,\\
b_{01}^{\rm E}&=b_{01}^{\rm L}\,,\\
b_{20}^{\rm E}&=\frac{8}{21}b_{10}^{\rm L}+b_{20}^{\rm L}\,,\\
b_{11}^{\rm E}&=b_{01}^{\rm L}+b_{11}^{\rm L}\,,\\
b_{02}^{\rm E}&=b_{02}^{\rm L}\,.
\end{aligned}$$

PNG with LSS: the galaxy bispectrum

We use the following standard definitions for the galaxy power spectrum P_{gg} and bispectrum B_{ggg}:

$$\langle \delta_g^{\rm E}(\mathbf{k}_1)\delta_g^{\rm E}(\mathbf{k}_2)\rangle = (2\pi)^3\delta^D(\mathbf{k}_1+\mathbf{k}_2)P_{gg}(\mathbf{k}_1)\,,$$
$$\langle \delta_g^{\rm E}(\mathbf{k}_1)\delta_g^{\rm E}(\mathbf{k}_2)\delta_g^{\rm E}(\mathbf{k}_3)\rangle = (2\pi)^3\delta^D(\mathbf{k}_1+\mathbf{k}_2+\mathbf{k}_3)B_{ggg}(\mathbf{k}_1,\mathbf{k}_2,\mathbf{k}_3)\,.$$

At tree-level, they can be conveniently written as

$$P_{gg}(\mathbf{k}_1) = E_1^2(\mathbf{k}_1)P(k_1)\,,$$
$$B_{ggg}(\mathbf{k}_1,\mathbf{k}_2,\mathbf{k}_3) = 2E_1(\mathbf{k}_1)E_1(\mathbf{k}_2)E_2(\mathbf{k}_1,\mathbf{k}_2)P(k_1)P(k_2) + 2 \text{ cyc.}\,,$$

where $P(k)$ is the matter power spectrum for the Gaussian source field φ_G, while the kernels E_i are defined as

$$E_1(\mathbf{k}_1) = b_{10} + \frac{b_{01}}{\alpha(k_1)}$$

→ scale-dependent bias term $\quad b_{01}/\alpha(k_1) \propto f_{\rm NL}/k_1^2$

$$E_2(\mathbf{k}_1,\mathbf{k}_2) = b_{10}\left[F_2(\mathbf{k}_1,\mathbf{k}_2) + f_{\rm NL}\frac{\alpha(|\mathbf{k}_1+\mathbf{k}_2|)}{\alpha(k_1)\alpha(k_2)}\right] + \left[b_{20} - \frac{2}{7}b_{10}^{\rm L}S_2(\mathbf{k}_1,\mathbf{k}_2)\right]$$
$$+ \frac{b_{11}}{2}\left[\frac{1}{\alpha(k_1)} + \frac{1}{\alpha(k_2)}\right] + \frac{b_{02}}{\alpha(k_1)\alpha(k_2)} - b_{01}\left[\frac{N_2(\mathbf{k}_1,\mathbf{k}_2)}{\alpha(k_2)} + \frac{N_2(\mathbf{k}_2,\mathbf{k}_1)}{\alpha(k_1)}\right]$$

PNG with LSS: Bispectrum

Sample	Power Spectrum		Bispectrum	
	$\sigma_{f_{\rm NL}}$ bias float	$\sigma_{f_{\rm NL}}$ bias fixed	$\sigma_{f_{\rm NL}}$ bias float	$\sigma_{f_{\rm NL}}$ bias fixed
BOSS	21.30	13.28	$1.04^{(0.65)}_{(2.47)}$	$0.57^{(0.35)}_{(1.48)}$
eBOSS	14.21	11.12	$1.18^{(0.82)}_{(2.02)}$	$0.70^{(0.48)}_{(1.29)}$
Euclid	6.00	4.71	$0.45^{(0.18)}_{(0.71)}$	$0.32^{(0.12)}_{(0.35)}$
DESI	5.43	4.37	$0.31^{(0.17)}_{(0.48)}$	$0.21^{(0.12)}_{(0.37)}$
BOSS + Euclid	5.64	4.44	$0.39^{(0.17)}_{(0.59)}$	$0.28^{(0.11)}_{(0.34)}$

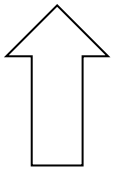

Tellarini et al. 2016

- Fisher matrix forecast. Tree-level bispectrum. Local NG initial conditions. In redshift space. Covariance between different triangles neglected (optimistic).
- The bispectrum could do better than the power-spectrum.
- $f_{NL} \sim 1$ achievable with forthcoming surveys?
- Many issues, e.g. full covariance, accurate bias model, GR effects, survey geometry, estimator implementation … Still, great potential: 3D vs 2D (CMB).

GR effects on the PS and bispectrum

- In full generality GR effects (including also redshift-space distortions, lensing, etc …) have to be taken into account both in the galaxy power-spectrum and bispectrum, as well as in the DM evolution.
- Recently, Bertacca, Raccanelli, Bartolo, Liguori, Matarrese & Verde (2017) obtained for the first time the complete expression for the galaxy bispectrum (which is obviously VERY complex) to be soon compared with observations.

Equilateral PNG: theoretical uncertainties

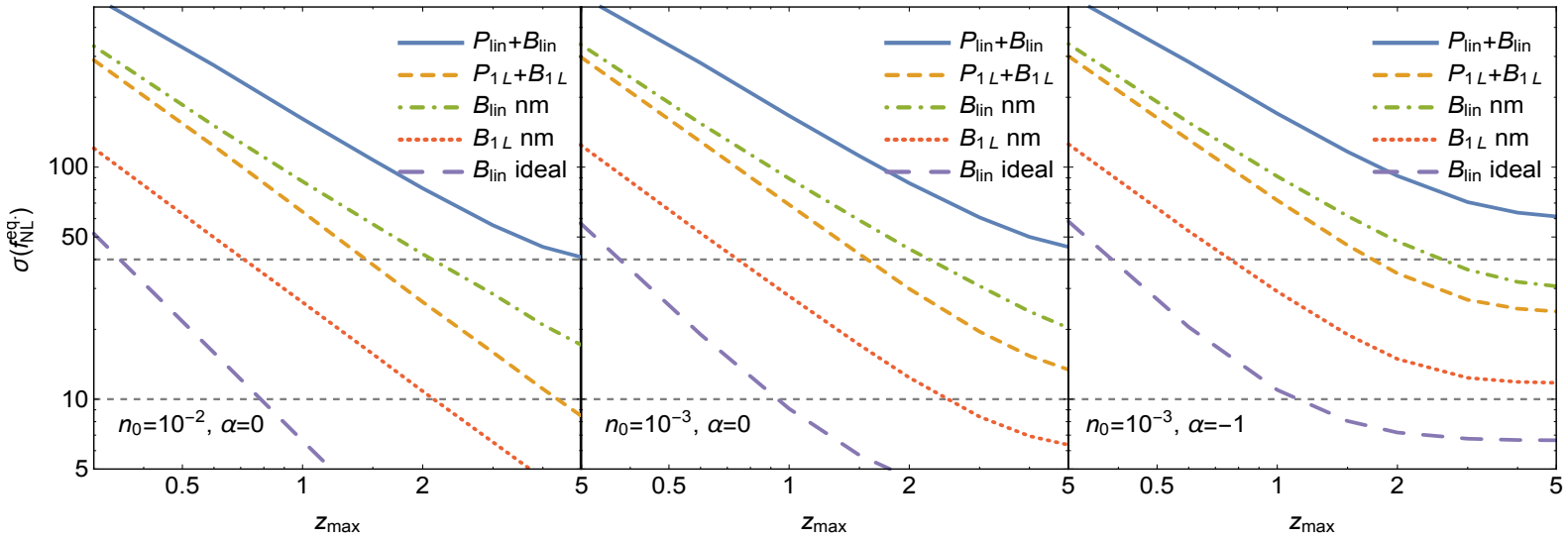

Baldauf et al. 2016

- The LSS bispectrum allows in principle tight constraints also on non-local shapes (e.g. equilateral)
- Naive mode counting suggest $\sigma_{fNL} \sim 1$ for equilateral might be achievable by pushing k_{max} high enough
- However, in the non-linear regime we have to model the gravitational bispectrum with high accuracy. Very challenging. Equilateral is more correlated than local to non-linear gravitational bispectrum, so bigger problem.

Credits: M. Liguori

Controversial issues on non-Gaussianity

Is the single-field consistency relation observable?

The cispectrum for single-field inflation (Gangui et al. 1995; Acquaviva et al. 2001; Maldacena 2001) can be represented as:

$$B_\zeta(k_1,k_2,k_3) \propto \frac{(\Delta^2_\zeta)^2}{(k_1k_2k_3)^2}\left[(1-n_s)\,\mathcal{S}_{\rm loc.}(k_1,k_2,k_3)+\frac{5}{3}\varepsilon\,\mathcal{S}_{\rm equil.}(k_1,k_2,k_3)\right]$$

$$n_s-1=-\eta-2\varepsilon,\ \text{with}\ \varepsilon\equiv-\frac{\dot H}{H^2},\ \eta\equiv\frac{\dot\varepsilon}{H\varepsilon}$$

The observability of the so-called "Maldacena consistency relation", related to the above bispectrum for single field inflation, in CMB and LSS data has led to a long-standing controversy. Recently, various groups have argued that the (1-n_s) term is totally unobservable (for single-clock inflation), as, in the *strictly squeezed limit* (one of the wave-numbers going to 0), this term can be gauged away by a suitable coordinate tranformation. Cabass, Schmidt and Pajer (2017) argued that the term survives up to a "renormalization" which further reduces it by a factor of ~ 0.1 if one applies Conformal Fermi Coordinates to get rid of such a "gauge mode".

- Is this (CFC approach) the only way to deal with this term?
- Can we aim at an **exact** description, which is not affected by "spurious PNG"?

f_{NL}-like effects from non-linear GR effects?

- Second order DM dynamics in GR leads to (post-Newtonian) **$\delta\,\zeta$** -like terms which mimic local primordial non-Gaussianity (Bartolo, Matarrese & Riotto 2005). Verde & Matarrese 2009 include this GR term in halo bias. The same GR term can be trivially recovered by a short-long mode splitting, leading to a resummed non-linear contribution **$\delta\, e^{-2\zeta}$** (Bruni, Hidalgo & Wands 2014). This comes from the modulation of sub-horizon scales due to modes entering the horizon at any given time.
- In the comoving gauge (suitable for calculation of halo bias) this would correspond to an $f_{NL} = -5/3$ in the pure squeezed limit.
- *Is such a GR NG signature detectable via some cosmological observables?*

f_{NL}-like terms generated by non-linear GR evolution

Poisson gauge

PNG-like GR (actually PN) terms

$$f_{\rm NL}^{P}(\mathbf{k}_1,\mathbf{k}_2;\tau) = \left[\frac{5}{3}(a_{\rm NL}-1)+1-\frac{g}{g_{\rm in}}-\frac{1}{2}\frac{B_1(\tau)}{gg_{\rm in}}\right]-\frac{(k_1^2+k_2^2)}{k^2}\frac{g}{g_{\rm in}}$$
$$+\frac{(\mathbf{k}_1\cdot\mathbf{k}_2)}{k^2}\left[\frac{2}{3}e(\tau)\frac{g}{g_{\rm in}}+\frac{1}{2}\frac{g}{g_{\rm in}}+\frac{2}{3}-\frac{1}{2}\frac{B_2(\tau)}{gg_{\rm in}}+\frac{3}{2}\mathcal{H}^2\frac{B_4(\tau)}{gg_{\rm in}}\right]$$
$$+\frac{(\mathbf{k}\cdot\mathbf{k}_1)(\mathbf{k}\cdot\mathbf{k}_2)}{k^4}\left[\frac{3}{2}\mathcal{H}^2\frac{B_3(\tau)}{gg_{\rm in}}-2+\frac{3}{2}\frac{B_2(\tau)}{gg_{\rm in}}\right]-\frac{(\mathbf{k}\cdot\mathbf{k}_1)(\mathbf{k}\cdot\mathbf{k}_2)}{k^2}\frac{k_1^2+k_2^2}{k_1^2k_2^2}$$
$$\times\frac{3}{2}\mathcal{H}^2 f(\tau)\frac{B_3(\tau)}{gg_{\rm in}}-(\mathbf{k}_1\cdot\mathbf{k}_2)\frac{k_1^2+k_2^2}{k_1^2k_2^2}\frac{3}{2}\mathcal{H}^2 f(\tau)\frac{B_4(\tau)}{gg_{\rm in}}.$$

Comoving and synchronous gauge

$$f_{\rm NL}^{C}(\mathbf{k}_1,\mathbf{k}_2) = \frac{5}{3}\left[(a_{\rm NL}-1)-1+\frac{5}{2}\frac{\mathbf{k}_1\cdot\mathbf{k}_2}{k^2}\right]$$

from: Bartolo, Matarrese, Pantano & Riotto 2010

Long and short modes

In each patch, the comoving spatial element is

$ds^2_{(3)} = e^{2\zeta}\,\delta_{ij}\,dx^i\,dx^j$

There is a global background which must be defined with respect to some scale λ_0, at least as large as all the other scales of interest, i.e., at least as large as our presently observable Universe. It is important to distinguish this from the scale of the separate universe patches, λ_P . This is large enough for each patch to be treated as locally homogeneous and isotropic, but patches must be stitched together to describe the long-wavelength perturbations on a scale $\lambda_L \gg \lambda_P$. Thus,

$\lambda_0 > \lambda_L \gg \lambda_P \gg \lambda_S$

The local observer in a separate universe patch cannot observe the effect of ζ_L , which is locally homogeneous on the patch scale λ_P . However, local coordinates can be defined only locally and the long mode curvature perturbation is observable through a mapping from local to global coordinates.

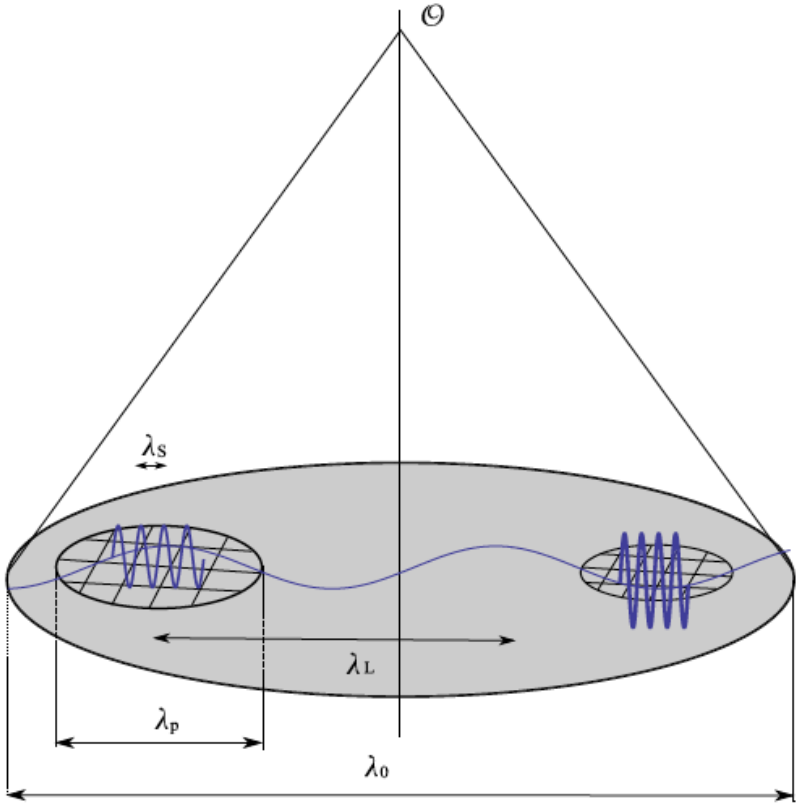

from: Bartolo et al. 2016

Observability of GR non-linearities

- In the halo bias case the effect is unobservable. Indeed, as pointed out by Dai, Pajer & Schmidt 2015 and de Putter, Doré & Green 2015, a local physical redefinition of the mass, gauges way such a NG effect (*in the pure squeezed limit*), similarly to Maldacena's $f_{NL} = -5/12(n_s-1)$ single-field NG contribution.

- This is true *provided the halo bias definition is strictly local*. Are there significant exceptions? Are all non-linear GR effects fully accounted for by "projection effects"?

- However, this dynamically generated GR non-linearity is physical and cannot be gauged away by any local mass-rescaling, provided it involves scales larger than the patch required to define halo bias, but smaller than the separation between halos (and the distance of the halo to the observer).

- Hence one would expect it to be in principle detectable in the matter bispectrum. Similarly, the observed galaxy bispectrum obtained via a full GR calculation must include all second-order GR non-linearities on such scales (*only as projection effects?*)

Beyond Separate Universes ...

- The Separate Universe approach proved very useful for many applications, but:
- The effect of the external world cannot be always described by linear theory → the usual identification large scales = linear theory is only qualitative and can become misleading in some cases: e.g. perturbations of order N >> 1 give the leading contribution to N-th order moments, such as $\langle\delta^N\rangle_c$. And, we know from non-linear Newtonian dynamics that $\langle\delta^N\rangle_c \sim \langle\delta^2\rangle^{N-1}$ on all scales (for scale-free spectra).
- Well inside a given Separate Universe assuming that the only non-linearity is described by Newtonian physics can be too restrictive. The relevance of non-linear GR effects in sub-patch dynamics depends upon the specific problem.
- It would be interesting to see the effects of using e.g. the Silent Universe description to account for deviations of the patch from purely spherical behavior (remember that over-dense patches evolve towards oblate ellipsoids; even under-dense ones can collapse to oblate ellipsoids, owing to tidal effects of surrounding matter).
- Interesting recent approach using Local Tide Approximation (Ip & Schmidt 2017) goes in this direction.

Concluding remarks

Short term goals

- Improve f_{NL} limits from CMB (*Planck*) with polarization & full data
- Look for more non-Gaussian shapes, scale-dependenf f_{NL}, etc. ...
- Make use of bispectrum in 3D data
- Improve constraints on g_{NL}

Long term goals

- reconstruct inflationary action
- if (quadratic) NG turns out to be small for all shapes go on and search for $f_{NL} \sim 1$ non-linear GR effects and second-order radiation transfer function contributions. For LSS resort to GR-based N-body simulations!

- ✓ Inflation provides a causal mechanism for the generation of cosmological perturbations
- ✓ CMB and LSS data fully support the detailed predictions of inflation
- ✓ The direct detection of:
  - ☞ primordial **gravitational waves**
  - ☞ primordial **non-Gaussianity**

  with the specific features predicted by inflation would provide strong independent support to the model